

## Revisiting strength concepts and correlations with soil index properties: insights from the Dobkovičky landslide in Czech Republic

**Abstract** Critical and residual states are key soil conditions relevant to slope stability. Evaluating the available shear strength in relation to these conditions is crucial for reliable stability analyses. However, limited availability of direct measurements in the usual engineering practice makes such evaluation seldomly straightforward. The issue is sometimes alleviated by utilising empirical correlations with soil index properties, more easily determinable, yet much care is needed in applying generic correlations to specific materials, as the related uncertainties might override their predictive capability. By analysing soil samples from the *Dobkovičky* landslide in Czech Republic, we discuss the extent to which some established correlations can be misleading, but also that relationships calibrated on site-specific data are not necessarily performing better. We then demonstrate that empirical models may fail to capture correlations if the sample set is rather homogeneous and noise from reasonable experimental uncertainties is introduced. Finally, we provide some guidelines on the use of different soil strength parameters, laboratory tests, and empirical relationships for slope stability analyses in engineering practice.

**Keywords** Residual shear strength · Critical state · Index properties · Empirical correlation · Slope stability · Partial saturation

### Introduction

#### The shear strength for stability analyses

The shear strength of soils can be expressed conventionally by the Mohr-Coulomb failure criterion:

$$\tau = c' + \sigma' \tan\phi' \quad (1)$$

where  $\tau$  and  $\sigma'$  are the shear and the effective normal stresses, respectively, and  $c'$  and  $\phi'$  are the effective cohesion intercept and the friction angle. Their values depend on the state (peak, critical, residual) and stress range under investigation. Values smaller than the peak ( $\phi_p$ ) are available in soils with important shear strain history, for which the critical state ( $\phi_{cr}$ ) or the residual ( $\phi_r$ ) friction angles might be more representative. Advanced constitutive models require additional parameters, calibrated through specific experiments (e.g. D'Onza et al. 2011; Hu et al. 2018). However, their use in slope stability assessments can be onerous and time consuming; thus, it is reserved to important projects, while only conventional, simplified analyses are performed in usual practice.

A critical state generally exists for any soil, while the residual strength is properly defined only in the clay-rich ones (Skempton 1985; Stark and Eid 1994; Leroueil 2001). When sheared to large strains, the soil loses its structure and bonding—imprinted by its formation and stress history—and reaches an ultimate constant-volume condition on

the critical state line (Schofield and Wroth 1968), with zero effective cohesion ( $c' = 0$ ) and a friction angle ( $\phi'_{cr}$ ) unique for the material. If clay-rich soils are sheared further, a further loss of strength may occur, with the clay platelets aligning in the direction of shearing (Skempton 1964), until a minimum value, the residual shear strength ( $\tau_r$ ), is attained.

Critical state and residual shear strengths in clay-rich soils, being independent of the soil's initial structure and stress history, could theoretically be obtained from undisturbed, remoulded, or reconstituted samples (cf. Burland 1990). However, for an accurate evaluation of the residual shear strength, the use of reconstituted samples is often the only viable option. In principle, some processes related to the preparation and testing of reconstituted samples (such as treating organic soils with strong acids, heavily milling crushable grains, or loading under very high stresses) might cause the response of some soils to differ from that in the undisturbed condition to some extent (see, e.g. Tengattini et al. 2016; Zhang et al. 2018). However, this is not the case for the soils that will be considered in this work (i.e. clay-rich materials subjected to effective stresses typical of landslide shear zones), neither it should represent an issue in the empirical correlations from the literature that we are going to investigate. It is worth noting that the procedure of sample reconstitution is well established in the literature, and has been commonly used in geotechnical practice even before Burland (1990)'s paper was published.

The evaluation of the effective stress in situ brings further complications to stability analyses, as it depends on local hydraulic conditions, and controls, in turn, the available strength. For instance, dry periods are conducive to negative pore pressures in shallow soil layers (suctions,  $s$ ), that play in favour of stability. With small suctions ( $s < s_e$ , where  $s_e$  is the air-entry value), the soil remains practically saturated, the water phase is continuous, and air and water pressures are approximately equal. A conventional undrained stability analysis for saturated soil can still be done using the undrained strength ( $s_U$ ), defined through the concept of state boundary surface:

$$s_U = \frac{1}{2} q_U = \frac{1}{2} M e^{\left(\frac{\Gamma - \gamma_0}{\lambda}\right)} \quad (2)$$

where  $q_U$  is the deviatoric stress at undrained failure, and  $M$ ,  $\Gamma$  and  $\lambda$  are parameters of the critical state line, determinable in the laboratory. Alternatively,  $s_U$  can be expressed through Hvorslev's equivalent pressure (i.e. through the parameters of the normal compression line). Some of the parameters can be estimated by theoretically well-justified correlations, bypassing laboratory testing.

If suction is large ( $s > s_e$ ), the soil loses saturation and variations in suction are related to capillary cohesion, which depends on the suction stress ( $\sigma_s$ ; Lu and Likos 2004). Figure 1a, in which the soil strength is assumed controlled by  $\phi'_{cr}$  exemplifies this

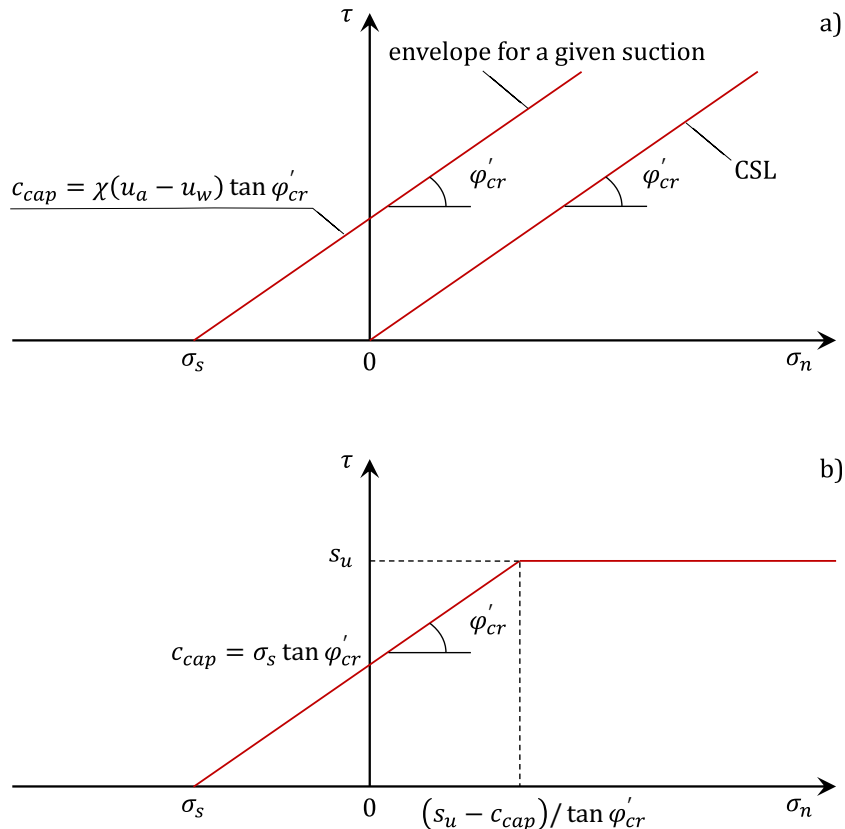


**Fig. 1** a Definition of capillary cohesion. b Simple concept for short-term stability analysis of unsaturated soil;  $\sigma_n$  is the net normal stress;  $\sigma_s = s\chi$  is the suction stress, where  $s = u_a - u_w$ , and  $u_a$  and  $u_w$  are the air and water pressures in the pores, respectively;  $c_{cap}$  is the capillary cohesion

condition. Khalili and Khabbaz (1998) showed that the effective stress concept can still be used, with  $\chi = (s_e/s)^\gamma$  and  $\gamma = 0.55$ . Mašín (2010) incorporated  $\chi$  in Brooks and Corey's (1964) water retention curve (WRC), showing that it can also be expressed through the degree of saturation as  $\chi = S_r^{(\gamma/\lambda_p)}$ , where  $\lambda_p$  is the slope of the WRC. If the strength is controlled by  $\phi'_{cr}$ , a strength envelope for variable saturation can be proposed (Fig. 1b), and the suction-induced capillary cohesion ( $c_{cap}$ ) can be written as:

$$c_{cap} = \sigma_s \tan \phi'_{cr} = s\chi \tan \phi'_{cr} = s \left( \frac{s_{eo} e_0}{e s} \right)^\gamma \tan \phi'_{cr} \quad (3)$$

where  $e$  and  $s$  are the current values of void ratio and suction, and  $s_{eo}$  is the suction at the reference void ratio  $e_0$ , determined from the WRC (Mašín 2010). Then,  $c_{cap}$  and  $\phi'_{cr}$  can be used in conventional total-stress, short-term stability analyses. For long-term analyses, the concept of effective stress for unsaturated soil can be used together with conventional solutions for drained loading, enabling simple slope stability assessments under seasonally varying saturation to be carried out.

#### Correlations for critical state and residual strengths

Numerous correlations have been established to estimate strength parameters of soils from simple index properties instead of performing laboratory shear tests. The critical state—an asymptotic state (Gudehus 2011; Mašín 2012) of the soil mechanical behaviour—is unique for a given mineralogy and shape of soil particles; hence, correlations with

other parameters should be relatively straightforward. Conversely, the residual strength depends upon additional factors, including viscous (time- and rate-dependent) properties and changes in pore water state (Gudehus 2011). Intuitively, it can be anticipated that correlations with index properties might be less reliable for the residual strength.

Several studies investigated relationships between shear strength parameters and the plasticity index ( $I_p$ ) of normally consolidated natural clays (e.g. Kenney 1959, Brooker and Ireland 1965; Ladd et al. 1977; Stark and Eid 1994; Terzaghi et al. 1996). The relationship between  $\phi'_{cr}$  and  $I_p$  and the decrease of  $\phi'_{cr}$  with the proportion of active clay minerals increasing were described, for instance, by Muir Wood (1990). Terzaghi et al. (1996) pointed out that the friction angle determined at a random arrangement of particles, often defined as the fully softened friction angle ( $\phi'_{fs}$ )—and referred to as the critical state friction angle (Burland 1990)—is a function of the content of clay minerals and their mineralogical composition. The authors reported values of  $\phi'_{fs}$  for a full range of  $I_p$  encountered in engineering practice. Sorensen and Okkels (2013) reviewed more than 200 tests from Ladd et al. (1977), with data from Kenney (1959), Bjerrum and Simons (1960), Terzaghi et al. (1996), and Brooker and Ireland (1965). Even though the authors observed a clear trend of  $\phi'_{nc}$  (the secant peak friction angle for normally consolidated soils, assuming  $c' = 0$ , which can be assumed as analogous to  $\phi'_{cr}$ ) decreasing with  $I_p$  increasing, this was accompanied by large scatter (e.g.  $\phi'_{nc} = 24\text{--}36^\circ$  for  $I_p = 30\%$ ).

First measurements of the strength of clayey soils after large shear strains were performed by Hvorslev (1937), Tiedemann (1937), and later by Terzaghi and Peck (1948), but it was Skempton (1964) who drew the attention to the significance of  $\phi'_r$  in the behaviour of landslides in clay-rich soils. He also proposed a correlation between  $\phi'_r$  and the clay fraction (*c. f.*, i.e. the proportion in dry weight of soil particles with size smaller than 2  $\mu\text{m}$ ), observing that, despite some scatter,  $\phi'_r$  decreased with the *c. f.* increasing. Such correlation was later observed by a number of researchers. Lupini et al. (1981) investigated the residual shear strength of mixtures of sands and clays with various mineralogy in various ratios. Further experiments were conducted, among others, by Mesri and Cepeda-Diaz (1986), Tiwari and Marui (2005) and Scaringi and Di Maio (2016). Kenney (1967) demonstrated that  $\phi'_r$  depends strongly on the mineral composition, particularly on that of the clay component, which can explain the scatter observed in Skempton's (1964)  $\phi'_r$ -*c. f.* correlation. Among others, Di Maio and Fenelli (1994) and Di Maio et al. (2015) pointed out also the importance of pore fluid chemistry, which can affect hydraulic conductivity, compressibility and strength dramatically. It was also recognised that mineralogy (Voight 1973) and pore fluid chemistry (Di Maio et al. 2004) affect the soil index properties (liquid limit  $w_L$ , plastic limit  $w_P$ , plasticity index  $I_P = w_L - w_P$ , activity  $A = I_P/c. f.$ ), implying that residual shear strength and index properties can be correlated. In fact, seeking correlations between strength parameters and index properties has been the object of numerous studies (e.g. Kanji 1974; Seyček 1978; Stark and Eid 1994; Kaya 2010; Ameratunga et al. 2016; Xu et al. 2018; Scaringi et al. 2018b). On the other hand, cases in which empirical correlations fail to describe the behaviour of some soils also have been reported (Wesley 2003; Tiwari and Marui 2005; Kaya and Kwong 2007).

The evaluation of index properties and the calibration of correlations with hydro-mechanical parameters are aimed at facilitating rapid assessments by professionals, especially when more advanced tests are not available in sufficient number or are impractical. Correlations can also be codified in regulations easily. However, the scattering in the data utilised to calibrate them should always be considered, and great care should be used with strength parameters derived from correlations rather than from shear tests. In this paper, we show, on the basis of experiments on samples from the Dobkovičky landslide (Czech Republic), to what extent existing correlations can yield unreliable predictions, but also that relationships calibrated on our data do not perform much better. We also discuss the role of uncertainties (often neglected in engineering practice) in the poor performance of some correlations, and we conclude by discussing some practical guidelines concerning the use of geotechnical tests and correlations in slope stability analyses.

## Materials and methods

### The Dobkovičky landslide

In June 2013, after heavy rains, a flow slide disrupted a highway under construction and a single-track railway near the village of Dobkovičky, Central Bohemian Uplands, Czech Republic (Fig. 2). The region suffers important slope deformations due to the intense Quaternary relief modelling by erosion and denudation,

abundance of weak soils, and seasonal variations of soil saturation and pore water pressures (Stemberk et al. 2016, Pospisil et al. 2019). The area of the Dobkovičky landslide mainly features outcrops from the upper Cretaceous, with abundance of tuff and claystone rich in smectite. Volcanic rocks and tuffs are associated with various types of volcaniclastic deposits (Cajz 2000), in which smectite-group minerals can be produced by alteration and weathering (e.g. De La Fuente et al. 2002). Slope deformations in the area are typically classified as planar slides or flow slides (see Hungr et al. 2014), occurring on slopes covered by soil mantles and colluvial deposits. The thickness of the landslide bodies (typically 2–10 m) is controlled by the depth at which the transition from colluvial deposits to weathered claystone occurs.

The Dobkovičky landslide body is about 200 m wide, 500 m long (Fig. 2b), and up to 8 m thick (4.5 m in average; Fig. 2d). It slid for about 50 m during 4 days, with a maximum rate of 1 m/h (Roháč et al. 2017). While the predisposing and triggering factors of the landslide remain object of discussion, Pospisil et al. (2019) suggested, on the basis of an archival study of technical reports carried out for the motorway construction (see also Pašek et al. 1972), that the landslide might have followed an older mapped slope deformation; therefore, it possibly moved over a preexisting shear zone with reduced strength.

After the slide, water ponds were observed in morphological depressions, and water springs emerged at the toe and remained active for some months, suggesting that the soil mass was saturated when the landslide occurred (Pospisil et al. 2019). Rainfall records at the site (Fig. 2e) show substantial variability in the pattern of precipitation. In summer, rainfall as low as 5 mm/month and as high as 280 mm/month were recorded. This variability might cause great variations in the depth of the groundwater table (possibly up to 25 m in the studied site; cf. Stemberk et al. 2016, Pospisil et al. 2019), as well as in the degree of saturation and pore water pressures in the soil layer. The proposed concept of soil strength at varying saturation ("The shear strength for stability analyses" section) is thus believed relevant for this case study. In most situations, the concept should use the critical state strength for "disturbed" (re-worked) soil. However, for re-activated landslides, the residual value may be relevant (see the comparison with back-analyses in "Comparison with results of back analyses" section). Employing the unsaturated soil concept in conventional slope stability analyses would have warned the designer that the apparent high strength and safety of the slope above the planned motorway was only associated to a relatively dry period. Upon saturation in the wet periods after 2010 (Fig. 2e), the strength decreased dramatically, which inevitably led to the failure of the unsupported excavation in 2013.

### Sampling and basic properties

Soil samples were obtained from borehole cores at three locations: 10 samples were extracted from the shear zone of the Dobkovičky landslide (Fig. 2c); 3 more (IND 204, IKC 12 and HG-C 1) from the surroundings (500–1000 m from the landslide), and additional 2 (J1 and J2) from the Výrovna landslide, about 20 km away. The soil strength and geological setting of the Výrovna landslide are analogous to those of the Dobkovičky landslide (see Valečka 1989, and "Laboratory shear tests" section). The natural water content ( $w$ ) was preserved in some cases (8 samples), for which an index of consistency,  $I_C = (w_L - w)/I_P$  of 1.03–1.35 was evaluated (i.e.  $w <$

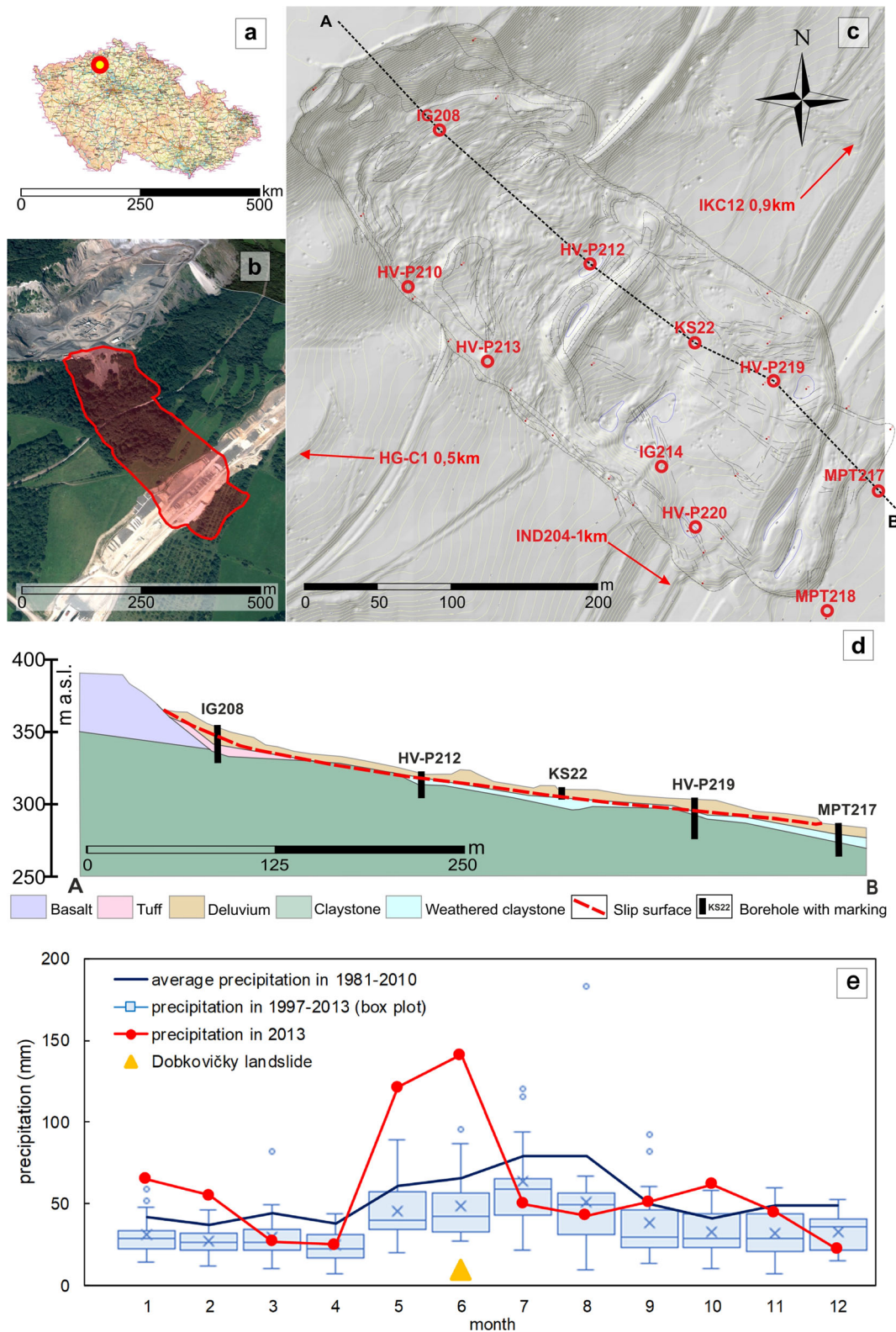


**Fig. 2** a Location of the Dobkovičky landslide in the Czech Republic. b Pre-landslide aerial view with indication of the landslide boundaries (source: ČÚZK – Czech Land Surveying and Cadastre Office). c Map of the landslide with location of boreholes. d Longitudinal profile of the landslide along section AB. e Monthly precipitation in 2013, compared with the 1981–2010 monthly average and statistics from 1997 to 2013. The box plots range from the 1st to the 3rd quartiles, the horizontal line is the median value, the cross marker is the average value, hollow markers are outliers (values above or below 1.5 times the interquartile range), and whiskers indicate the minimum and maximum values within the interquartile range. Precipitation data were recorded at Ústí nad Labem, 13 km from the Dobkovičky landslide by the Czech Hydrometeorological Institute

$w_p$ ). The grain size distributions of the samples are summarised in Fig. 3: most of them can be classified as clays and silts with sand. The index properties were determined following the ISO 17892-12 (2004) standard and are summarised in Table 1, together with the USCS classification of the samples (ASTM D-2487 2011). The apparently unrealistic value of activity ( $A = 7.7$ ) of sample HG-C 1 was discarded in the analyses initially, as the very low  $c.f. = 2\%$  was attributed to incomplete disaggregation prior to testing.

#### Laboratory shear tests

We prepared reconstituted samples by mixing the finely crushed and sieved (through 2 mm sieve) soil with distilled water to obtain a homogeneous slurry with  $w_o \approx 1.5w_L$  (Burland 1990). The critical state and the residual shear strengths were determined, respectively, in a conventional triaxial apparatus and in a ring shear apparatus (Bromhead 1979).

Triaxial samples (38 mm in diameter, 76 mm high) were prepared by one-dimensionally pre-consolidating the slurry under a vertical stress of 60 kPa. In the triaxial cell, radial filter paper drains were used, and after isotropic consolidation to cell pressures of 60, 120, or 200 kPa, the specimens were sheared in undrained condition, measuring pore pressures at the bottom of the specimens (CIUP tests). The shearing was strain-controlled, at a rate of axial displacement set at half of the value suggested by the ISO 17892-9 (2004).

The residual shear strength was determined on samples consolidated from the slurry under  $\sigma'_v = 30, 50, 70$  kPa. These values were chosen as representing the vertical stresses in the shear zone in situ. Displacement-controlled testing was performed at a fixed rate  $v = 0.045\text{mm/min}$ , after the effect of the rate of shear displacement was assessed on 2 samples with different  $I_p$  (in the range  $v = 0.018 - 44.5\text{mm/min}$ , under  $\sigma'_v = 50$  kPa), and on a commercial bentonite and a commercial sand, for comparison.

#### Empirical estimates of strength parameters

We obtained estimates of  $\phi'_{cr}$  and  $\phi'_r$  from the  $I_p$  of the tested soils by means of several empirical correlations from the literature:

$$\phi'_{cr} = 0.81 - 0.223 \log I_p \text{ Kenney (1959)} \quad (4)$$

$$\sin \phi'_{cr} = 0.35 - 0.1 \ln(I_p/100) \text{ Muir Wood (1990)} \quad (5)$$

$$\phi'_r = 46.6 I_p^{-0.446} \text{ Kanji (1974)} \quad (6)$$

$$\phi'_r = 47.76 e^{-0.022 I_p} \text{ Xu et al. (2018)} \quad (7)$$

where  $\phi'_{cr}$  is given in radians in Eq. (4),  $\phi'_r$  is in degrees in Eqs. (6) and (7), and  $I_p$  is in percentage everywhere. We selected these expressions because of their widespread use and large datasets over which they were calibrated (Kenney 1959; Kanji 1974; Muir Wood 1990), and/or for the simplicity of their expression (Kanji 1974; Xu et al. 2018), but also to show how they can yield values significantly different from each other.

Kenney (1959) obtained a correlation between the effective friction angle and the plasticity index based on a large number of triaxial tests on normally consolidated clays. Muir Wood (1990) obtained a similar correlation by interpreting a large dataset from Mitchell (1976), complemented with data from Brooker and Ireland (1965), all obtained on normally consolidated clays. For both Kenney's (1959) and Muir Wood's (1990) correlations, we assumed that the friction angles reported by the authors could be assimilated to critical state friction angles. Kanji (1974) derived a correlation between the residual friction angle and the plasticity index on the basis of direct shear tests on soils with a wide range of plasticity, including monomineralic clays and various natural soils, under consolidation stresses  $\sigma'_v = 10 - 350$  kPa. More recently, Xu et al. (2018) obtained a correlation from the results of ring shear experiments on various clay

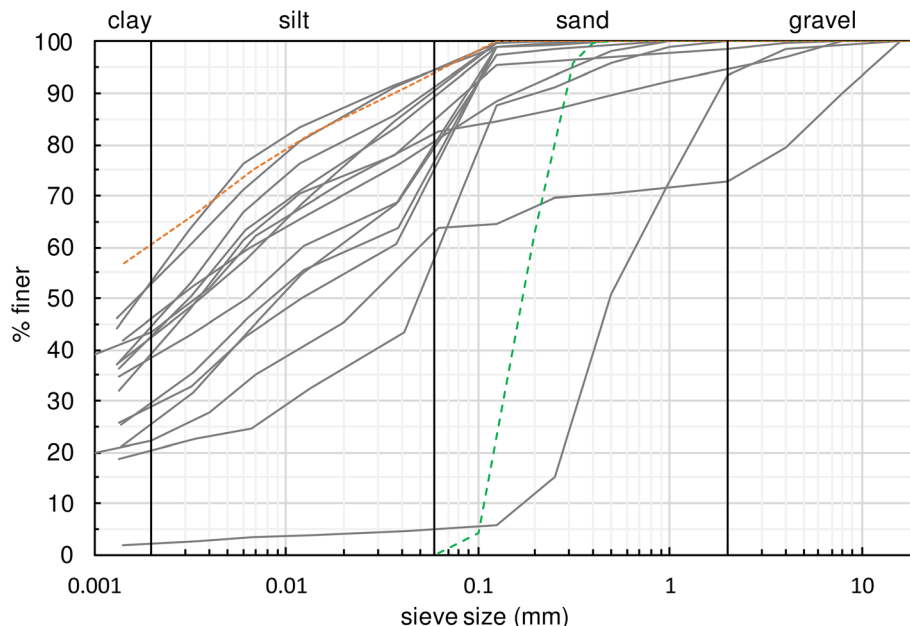


**Fig. 3** Grain size distributions of the tested samples. Solid grey lines for Dobkovický and Výrovna samples, dotted green line for the commercial bentonite and dashed orange line for the sand (see Table 1)

**Table 1** Grain size fractions (Gr = gravel, Sa = sand, Si = silt, Cl = clay) in dry weight, USCS classification (CL = clay of low plasticity, CH = clay of high plasticity, MH = silt of high plasticity, SP = poorly graded sand), index properties ( $w_L$ ,  $w_P$ ,  $I_P$ ,  $A$ ), and strength parameters ( $\phi'_{cr}$ ,  $\phi'_r$ ) of the tested samples. An asterisk (\*) denotes an unrealistic value of  $A$  due to a possibly underestimated  $c$ ,  $f$ .

| Location             | Sample   | Depth (m) | Grain size Gr/Sa/Si/Cl (%) | USCS  | $w_L$ (%) | $w_P$ (%) | $I_P$ (%) | $A$   | $\phi'_{cr}$ (°) | $\phi'_r$ (°) |
|----------------------|----------|-----------|----------------------------|-------|-----------|-----------|-----------|-------|------------------|---------------|
| Dobkovičky           | IND 204  | 10.8      | 0/6/40/54                  | CL    | 49.0      | 22.1      | 26.9      | 0.5   | 25.7             | 14.6          |
| Dobkovičky           | IG 208   | 6.5       | 0/42/38/20                 | MH    | 72.8      | 49.3      | 23.5      | 1.2   | 29.5             | 15.3          |
| Dobkovičky           | HV-P 210 | 5.6       | 0/9/49/42                  | CH    | 71.4      | 32.7      | 38.7      | 0.9   | 25.0             | 11.2          |
| Dobkovičky           | HV-P 212 | 2.3       | 0/8/47/45                  | MH    | 58.1      | 32.2      | 25.9      | 0.6   | 25.1             | 13.3          |
| Dobkovičky           | HV-P 213 | 2.5       | 0/6/41/53                  | CH    | 68.1      | 31.7      | 36.4      | 0.7   | 24.6             | 13.5          |
| Dobkovičky           | IG 214   | 7.5       | 0/18/36/46                 | CH    | 74.5      | 30.2      | 44.3      | 1.0   | 26.3             | 13.2          |
| Dobkovičky           | MPT 217  | 10.2      | 0/11/46/43                 | MH    | 64.4      | 33.2      | 31.2      | 0.7   | 24.2             | 12.4          |
| Dobkovičky           | MPT 218  | 10.1      | 2/13/46/39                 | CH    | 62.3      | 30.9      | 31.4      | 0.8   | 24.7             | 11.7          |
| Dobkovičky           | HV-P 219 | 6.5       | 0/23/47/30                 | MH    | 70.3      | 37.7      | 32.6      | 1.1   | 24.4             | 13.3          |
| Dobkovičky           | HV-P 220 | 8.3       | 0/24/47/29                 | CH    | 70.8      | 31.8      | 39.0      | 1.3   | 25.7             | 12.3          |
| Dobkovičky           | KS 22    | 2.6       | 0/20/42/38                 | MH    | 88.0      | 44.2      | 43.8      | 1.2   | 21.8             | 12.5          |
| Dobkovičky           | IKC 12   | 33.2      | 0/20/54/26                 | CH    | 58.1      | 30.3      | 27.8      | 1.1   | 26.6             | 12.7          |
| Dobkovičky           | HG-C 1   | 34.5      | 7/88/3/2                   | SP    | 61.9      | 46.6      | 15.3      | 7.7 * | 31.7             | 22.0          |
| Výrova               | J1       | 16.4      | 27/10/41/22                | CH    | 51.0      | 27.0      | 24.0      | 1.1   | —                | 12.4          |
| Výrova               | J2       | 9.0       | 6/12/39/43                 | CH    | 54.0      | 30.0      | 24.0      | 0.6   | —                | 12.1          |
| commercial bentonite |          | 0/6/33/61 | CH                         | 217.3 | 51.2      | 166.1     | 2.7       | —     | 6.9              |               |
| commercial sand      |          | 0/100/0/0 | SP                         | —     | —         | —         | —         | 34.9  | —                |               |

soils with  $I_p \leq 45\%$ , under  $\sigma'_v = 50\text{--}150\text{ kPa}$ . Here,  $c' = 0$  is considered for both the critical and residual strength envelopes, so that  $\tau_i$  can be obtained from the correlations as  $\tau_i = \sigma' \tan \phi'_i$  (with  $i$  indicating either the critical or the residual strength; cf. also Stark et al. 2005; Stark and Hussain 2013).

In addition, we used a group of more elaborate correlations from Stark and Hussain (2013) (Eqs. (8)–(13), and Table 2) that relate  $\phi'_{cr}$  and  $\phi'_r$  with  $w_L$  in various ranges of  $c.f.$  and  $w_L$ , under  $\sigma'_v$  values as close as possible to the experimental ones.

$$\phi'_{cr} = 34.39 - 0.0863 w_L + 2.66 \cdot 10^{-4} w_L^2 \quad (8)$$

$$\phi'_{cr} = 33.11 - 0.107 w_L + 2.2 \cdot 10^{-4} w_L^2 \quad (9)$$

$$\phi'_{cr} = 31.17 - 0.142 w_L + 4.678 \cdot 10^{-4} w_L^2 - 6.762 \cdot 10^{-7} w_L^3 \quad (10)$$

$$\phi'_r = 39.71 - 0.29 w_L + 6.63 \cdot 10^{-4} w_L^2 \quad (11)$$

$$\phi'_r = 31.4 - 6.79 \cdot 10^{-3} w_L - 3.616 \cdot 10^{-3} w_L^2 + 1.864 \cdot 10^{-5} w_L^3 \quad (12)$$

$$\phi'_r = 33.5 - 0.31 w_L + 3.9 \cdot 10^{-4} w_L^2 + 4.4 \cdot 10^{-6} w_L^3 \quad (13)$$

These correlations were obtained through ring shear tests on a large number of natural soils (73 for  $\phi'_r$  and 39 for  $\phi'_{cr}$ ; Stark and Eid 1994; Stark et al. 2005), under  $\sigma'_v = 50\text{--}700\text{ kPa}$  (Gamez and Stark 2014 later provided additional correlations for  $\sigma'_v = 12\text{ kPa}$ ). It is worth noting that Stark and Hussain (2013) did not actually refer to  $\phi'_{cr}$  directly, but to the fully softened friction angle  $\phi'_{fs}$ . The latter was evaluated in the ring shear apparatus and then corrected, on the basis of further tests conducted by the authors, to become representative of strength values evaluated in the triaxial apparatus. The authors suggested, however, following Skempton's definition (Skempton 1970, 1977; see also Take and Bolton 2011) that their  $\phi'_{fs}$  in normally consolidated clays can be a good approximation of  $\phi'_{cr}$ .

After analysing the values of  $\phi'_{cr}$  and  $\phi'_r$  obtained with the correlations from the literature—by discussing their coefficient of determination ( $R^2 = 1 - SS_{res}/SS_{tot}$ , where  $SS_{res}$  is the variance

of residuals and  $SS_{tot}$  is the total variance), the level of significance ( $p$  value,  $p$ ), and the deviation of the estimates from the experimental values—we calibrated new correlations using our own dataset. We did so by means of power law fittings in the form  $Y = aX^b$ , where  $X$  is an index property,  $Y$  is a strength parameter,  $a$  is an empirical multiplier, and  $b$  is an empirical exponent. Here, we should note that the purpose of these “site-specific” analyses is not to provide correlations with general validity, but to demonstrate the control exerted by the limited, site-specific set of experimental data (and the related uncertainties) on the evaluation and usability of such correlations, thus offering a critical view on the use of empirically-estimated strength parameters for stability analyses.

Finally, we further explored correlations between index properties and  $\phi'_r$  using an evolutionary solver, that identifies optimised global solutions to the problem of maximising  $R^2$ . The solver is provided in the *Solver add-in* program (Frontline Systems Inc., USA) and is implemented in a spreadsheet (Baker and Camm 2005; Baker 2011). The multipliers and the exponents in the power laws were constrained to  $[-500, 500]$  and  $[-2, 2]$ , respectively. With the latter choice, linear models ( $b = 1$ ), parabolic models ( $b = 2$ ), square root models ( $b = 0.5$ ), and hyperbolic models ( $b = -1$ ) are also contemplated, albeit without allowing for translation of axes.

## Results

### Laboratory shear tests

By performing CIUP triaxial tests on 13 samples (39 data points; Fig. 4), we obtained  $\phi'_{cr}$  values of  $22\text{--}32^\circ$  ( $26^\circ$  in average,  $R^2 = 0.91$ ,  $p < 0.001$ ,  $SD = 3.2^\circ$ , assuming a linear envelope with the constraint  $c' = 0$ ). Sample HG-C 1, having the lowest plasticity ( $I_p = 15.3\%$ ; Table 1), exhibited the highest  $\phi'_{cr}$ . Sample KS 22, with the highest liquid limit ( $w_L = 88\%$ ) and one of the highest plasticity index ( $I_p = 43.8\%$ ), exhibited the lowest  $\phi'_{cr}$ .

We performed ring shear tests on 15 samples (45 data points; Fig. 5a), which resulted in  $\phi'_r$  values of  $11\text{--}15^\circ$ . HG-C 1 was an exception ( $\phi'_r = 22^\circ$ ) as it is actually mostly constituted by sand (Table 1). By performing a regression analysis between  $\sigma'_v$  and  $\tau_r$ , assuming a linear envelope and  $c' = 0$ , we obtained an average  $\phi'_r$  of  $\sim 13.9^\circ$  ( $R^2 = 0.57$ ,  $p < 0.001$ ,  $SD = 2.6^\circ$ ), which became  $\sim 13.4^\circ$  ( $R^2 = 0.73$ ,  $p < 0.001$ ,  $SD = 1.7^\circ$ ) when HG-C 1 was excluded.

It is worth noting that a Z-test on the distribution of  $\phi'_r$  values of the samples from the Výrovna landslide, against those of the samples from the Dobkovičky landslide, yielded a z-score of 1.54, which is associated to a 2-tailed  $p$  value of 0.12, which confirms

**Table 2** Conditions for the applicability of the empirical correlations proposed by Stark and Hussain (2013) utilised in this study

| Equation | Valid for    | Reference $\sigma'_v$ | Range of $c.f.$ | Range of $w_L$ |
|----------|--------------|-----------------------|-----------------|----------------|
| (8)      | $\phi'_{cr}$ | 100 kPa               | $\leq 20\%$     | 30–80%         |
| (9)      | $\phi'_{cr}$ | 100 kPa               | 25–45%          | 30–130%        |
| (10)     | $\phi'_{cr}$ | 100 kPa               | $\geq 50\%$     | 30–300%        |
| (11)     | $\phi'_r$    | 50 kPa                | $\leq 20\%$     | 30–80%         |
| (12)     | $\phi'_r$    | 50 kPa                | 25–45%          | 30–130%        |
| (13)     | $\phi'_r$    | 50 kPa                | $\geq 50\%$     | 30–120%        |

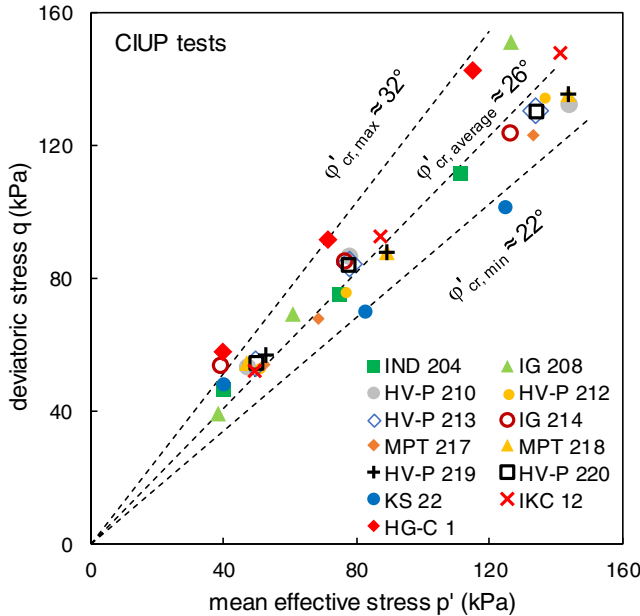


Fig. 4 Critical state envelopes of 13 soil samples tested in the triaxial apparatus

that, at a level of significance  $p = 0.05$ , the null hypothesis that the  $\phi'_r$  of the two landslide materials come from the same population (i.e. they are statistically the same) cannot be rejected.

In Fig. 5b, we analysed the correlation between  $\phi'_r$  and  $\phi'_{cr}$ . By hypothesising a linear correlation with zero intercept, we obtained a ratio  $\phi'_r/\phi'_{cr}$  of  $\sim 0.53$  ( $R^2 = 0.55$ ,  $p < 0.005$ ), with a standard deviation of the ratio  $SD = 0.06$ . If an intercept is permitted, the ratio  $\phi'_r/\phi'_{cr}$  becomes  $\sim 0.90$ , and a negative intercept of approx.  $-9.42^\circ$  is obtained ( $R^2 = 0.66$ ,  $p < 0.001$ ). This intercept does not have a physical meaning, and it is clear that the relation can only be used within the range of the experimental data. The correlation is sensitive to the strength values of sample HG-C1. If these values are excluded, we obtain a ratio  $\phi'_r/\phi'_{cr}$  of  $\sim 0.51$  and a standard deviation of the ratio  $SD = 0.038$  under the hypothesis of zero intercept, yet the quality of the correlation is far worse ( $R^2 = 0.26$ ,  $p < 0.1$ ) because of the reduced variability of the sample set. If an intercept is allowed, the correlation remains unsatisfactory, with a ratio  $\phi'_r/\phi'_{cr}$  of  $\sim 0.36$  and an intercept of  $\sim 3.92^\circ$  ( $R^2 = 0.32$ ,  $p < 0.1$ ).

#### Empirical estimates of strength parameters

A summary of the estimates obtained using correlations from the literature is given in Fig. 6. The correlations formulated in terms of  $I_p$  by Kenney (1959) and Muir Wood's (1990) overestimate the measured values of  $\phi'_{cr}$ , on average by  $1.6^\circ$  and  $2.1^\circ$ , respectively. The correlations with  $w_L$  and *c. f.* (for  $\sigma'_v = 100$  kPa) proposed by Stark and Hussain (2013) also overestimate the experimental  $\phi'_{cr}$  values by  $1.1^\circ$ . Actually, the three correlations yield consistent results: compared with the experimental results, they show similar coefficients of determination ( $R^2 = 0.42$ ,  $0.35$ ,  $0.46$  at  $p < 0.02$ ,  $0.05$ ,  $0.01$ , respectively) highlighting moderate performance but significant correlation. Moreover, a Z-test on the three sets of estimates highlights that the three correlations do not yield statistically

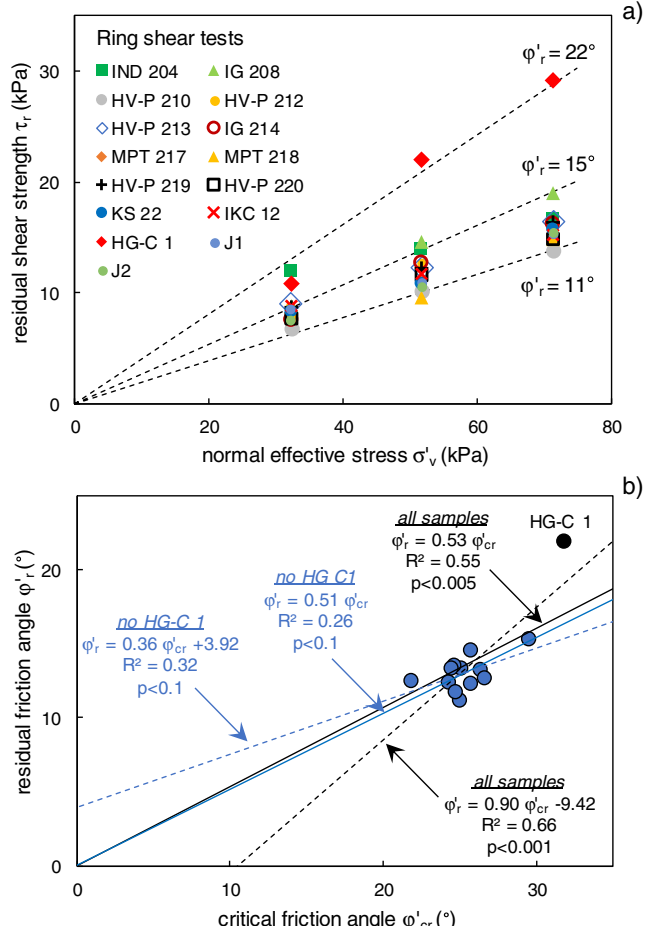
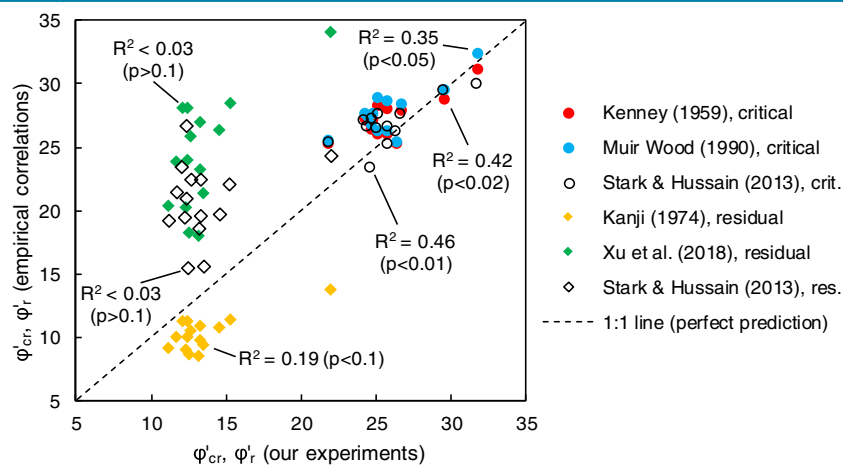


Fig. 5 a Residual shear strength envelopes for 15 soil samples tested in the ring shear apparatus. b Correlations between critical state (determined in CIUP triaxial tests) and residual friction angles

different results in our data set:  $p > 0.40$  between Kenney's (1959) and Muir Wood's (1990) estimates;  $p > 0.40$  between Kenney's (1959) and Stark and Hussain's (2013) estimates;  $p > 0.15$  between Muir Wood's (1990) and Stark and Hussain's (2013) estimates.

Worse performances are observed in predicting  $\phi'_r$ . The correlation in terms of  $I_p$  by Kanji (1974) underestimates  $\phi'_r$  by  $3.2^\circ$  on average. Compared with the experimental results, it has  $R^2 = 0.19$  at a level of significance  $p < 0.10$ , indicating only a small ability to predict the variance in the data set and a weak correlation with them. The correlations with  $I_p$  by Xu et al. (2018) and with  $w_L$  and *c. f.* by Stark and Hussain (2013) perform worse. The former overestimates  $\phi'_r$  by  $11^\circ$ , on average, while the latter overestimate it by  $7^\circ$ . Neither of them is significantly correlated with the experimental data ( $p > 0.10$ ) nor can explain their variance ( $R^2 < 0.03$ ). The correlation by Xu et al. (2018) is possibly biased by the calibration set of the authors, which only covered a small variety of soil types (cf. also Scaringi et al. 2018b), whose clay component and activity were smaller than in our samples. As for the correlations of Stark and Hussain (2013), we verified that using the relationships for  $\sigma'_v = 100$  kPa rather than for  $\sigma'_v = 50$  kPa does not improve the results significantly (the overestimation is still of about  $6^\circ$ ). Again, it is possible



**Fig. 6** Critical state and residual friction angles estimated from empirical correlations from Kenney (1959), Kanji (1974), Muir Wood (1990), Stark and Hussain (2013) and Xu et al. (2018), compared to the experimental values (cf. Figs. 4 and 5). Coefficients of determination ( $R^2$ ) and levels of significance (p-values) are indicated near each dataset

that the set of natural soils utilised by the authors to calibrate their relationships is not representative of the composition of our samples (possibly in terms of mineralogy of the clay component).

By calculating the standard deviations of the estimates ( $SD_{est.}$ ) obtained with the empirical correlations from the literature with respect to our experimental data, we can assess to what extent these correlations can provide estimates that are usable, for instance, in stability analyses. Assuming that the deviations follow a normal distribution centred around the average value, we can infer, with 68% confidence (i.e.  $\pm 1 SD_{est.}$  interval), that: Stark and Hussain's (2013), Kenney's (1959), and Muir Wood's (1990) correlations provide values of  $\phi'_{cr}$  within  $1.9^\circ$ ,  $2.2^\circ$  and  $2.5^\circ$  from the measured values, respectively, and Kanji's (1974), Stark and Hussain's (2013), and Xu et al.'s (2018) correlations provide values of  $\phi'_r$  within  $3.5^\circ$ ,  $8.0^\circ$  and  $11.5^\circ$  from the measured values. The deviations are twice as large if the interval  $\pm 2 SD_{est.}$  is considered, which corresponds to a level of confidence of 95%. As an exercise, considering that our experiments yield  $\phi'_{cr} = 25.8^\circ$  and  $\phi'_r = 13.5^\circ$ , on average, we can also infer ( $p < 0.05$ ) that Stark and Hussain's (2013) estimates of  $\phi'_{cr}$  carry a relative error  $< 15\%$ , which could be acceptable in preliminary stability analyses. Using Kenney's (1959) or Muir Wood's (1990) correlations, the error on  $\phi'_{cr}$  is  $< 17\%$  and  $< 20\%$  ( $p < 0.05$ ), respectively, which again might be acceptable. As for  $\phi'_r$ , we only can infer ( $p < 0.05$ ) that the error we can make is  $< 54\%$  using Kanji's (1974) correlation, which is evidently a poor constraint. Worse results, obviously, come from the use of Stark and Hussain's (2013) and Xu et al.'s (2018) correlations for  $\phi'_r$  on our dataset (relative error  $\sim 100\%$ ).

The inconsistency and dispersion of the strength parameters estimates, and the significant differences with the values determined by laboratory tests, demand further investigation on the correlations between soil index parameters and strength parameters. Figure 7 a shows the correlations of  $A$  and  $c.f.$  with  $\phi'_{cr}$  and  $\phi'_r$ , while Fig. 7b shows those of  $w_L$ ,  $w_P$  and  $I_P$  with  $\phi'_{cr}$  and  $\phi'_r$ . In general, index properties can

explain only a small or moderate portion of the variance in friction angles observed in the data:  $c.f.$  correlates with  $\phi'_r$  very weakly and with low significance ( $R^2 = 0.15$ ,  $p > 0.1$ ), while a slightly stronger and significant correlation is found with  $\phi'_{cr}$  ( $R^2 = 0.29$ ,  $p < 0.07$ );  $w_P$  does not provide much information on the variance of  $\phi'_r$  and  $\phi'_{cr}$  ( $R^2 < 0.01$ ,  $p > 0.1$ , and  $R^2 = 0.12$ ,  $p > 0.1$ , respectively); almost no correlation is observed between  $w_L$  and  $\phi'_{cr}$  ( $R^2 = 0.09$ ,  $p > 0.1$ ), while some correlation is found between  $w_L$  and  $\phi'_r$  ( $R^2 = 0.24$ ,  $p < 0.05$ ).

Interestingly, but expected from the literature, if the plasticity index ( $I_P = w_L - w_P$ ) is considered, stronger and more significant correlations are obtained ( $R^2 = 0.64$ ,  $p < 0.001$  with  $\phi'_{cr}$ , and  $R^2 = 0.68$ ,  $p < 0.001$  with  $\phi'_r$ ). These correlations permit  $\phi'_{cr}$  and  $\phi'_r$  estimates within  $1.9^\circ$  and  $1.7^\circ$  from the experimental values, respectively, with 68% confidence ( $\pm 1 SD$  interval), or within  $3.8^\circ$  and  $3.4^\circ$ , respectively, with 95% confidence ( $\pm 2 SD$  interval). However, while  $I_P$  is a good (independent) variable, activity ( $A = I_P/c.f.$ ) performs much worse: in fact, while a significant correlation is still found between  $A$  and  $\phi'_r$  ( $R^2 = 0.35$ ,  $p < 0.02$ ), no correlation is found between  $A$  and  $\phi'_{cr}$  in our dataset ( $R^2 < 0.02$ ,  $p > 0.1$ ).

The correlation between  $I_P$  and the residual shear strength ( $\tau_r$ ) was explored further by considering its dependence to  $\sigma'_v$  explicitly (i.e., a non-linear strength envelope; cf. “The shear strength for stability analyses” section). In Fig. 7c,  $\tau_r$  values obtained under different  $\sigma'_v$  were fitted by an effective normal stress-dependent power law, the coefficients of which (identical for all  $\sigma'_v$  values) were chosen in such a way to maximise the overall coefficient of determination ( $\sum R^2$ ). It is interesting to notice that this best fit relationship produces lower coefficients of determination at each normal stress ( $R^2 = 0.37$  under  $\sigma'_v = 70kPa$ ,  $R^2 = 0.33$  under  $\sigma'_v = 50kPa$ , and  $R^2 = 0.30$  under  $\sigma'_v = 30kPa$ , with levels of significance  $p < 0.02$ ,  $0.05$ ,  $0.05$ , respectively; Fig. 7c) than that obtained with  $\phi'_r$  ( $R^2 = 0.68$ ,  $p < 0.001$ ; Fig. 7b) independently of the  $\sigma'_v$  values. This might have to do with a non-linearity of the residual strength envelope at low  $\sigma'_v$  but also to the possibility that power law fittings are not the most suited to the specific problem.

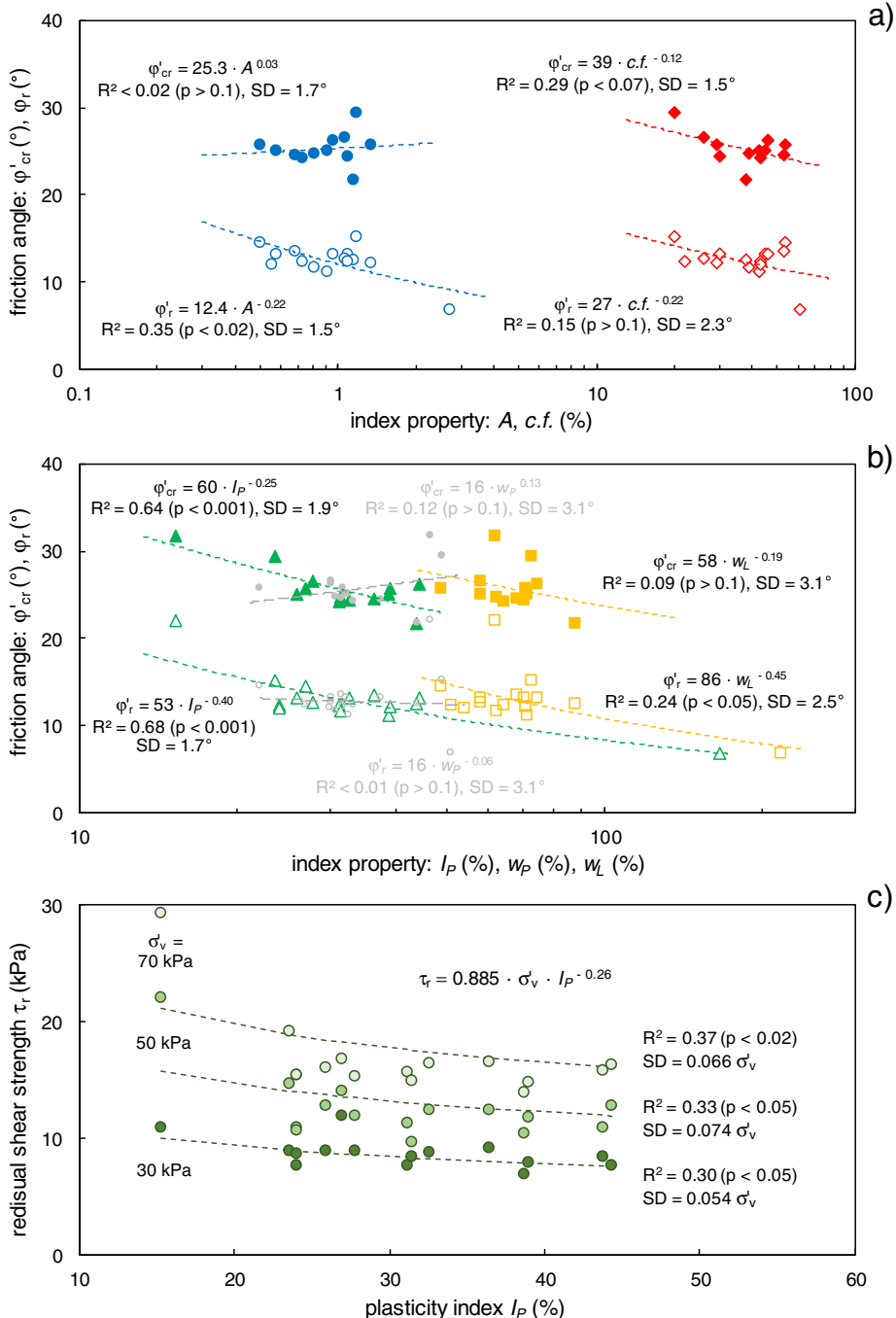


**Fig. 7** Correlations between  $\phi'_c$  or  $\phi'_r$  and index properties: a  $A$ ,  $c.f.$ ; b  $I_P$ ,  $w_P$ ,  $w_L$ . Correlation between  $\tau_r$  and  $I_P$  (c). Data refer to the 15 samples from Dobkovičky and Výrovna landslides, and to the commercial bentonite (cf. Table 1). Empirical power-law fittings are obtained, for which the coefficient of determination  $R^2$ , the level of significance  $p$ , and the standard deviation SD between experimental and predicted values of  $\phi'_r$  are reported. Note that sample HG-C 1 was excluded from the correlations in a due to its very low  $c.f.$  and consequent unrealistic  $A$

We have explored the correlations between index properties and  $\phi'_r$  further by means of an evolutionary solver to identify optimal solutions (cf. “**Empirical estimates of strength parameters**” section). The results of the optimisation analyses are shown in Fig. 8. In particular, in Fig. 8a, b, c and g, the same training set has been used, which includes all landslide soil

samples (cf. Table 1) except HG-C 1. Optimised correlations have been sought with  $c.f.$  (Fig. 8a),  $I_P$  (Fig. 8b) and  $A$  (Fig. 8c), obtaining values of  $R^2$  similar to those shown in Fig. 7, but not identical (also because HG-C 1 had not been excluded in the fittings in Fig. 7b). It is again shown that the best individual predictor for  $\phi'_r$  is  $I_P$  ( $R^2 = 0.647$ ,  $p < 0.001$ ; Fig. 8b),

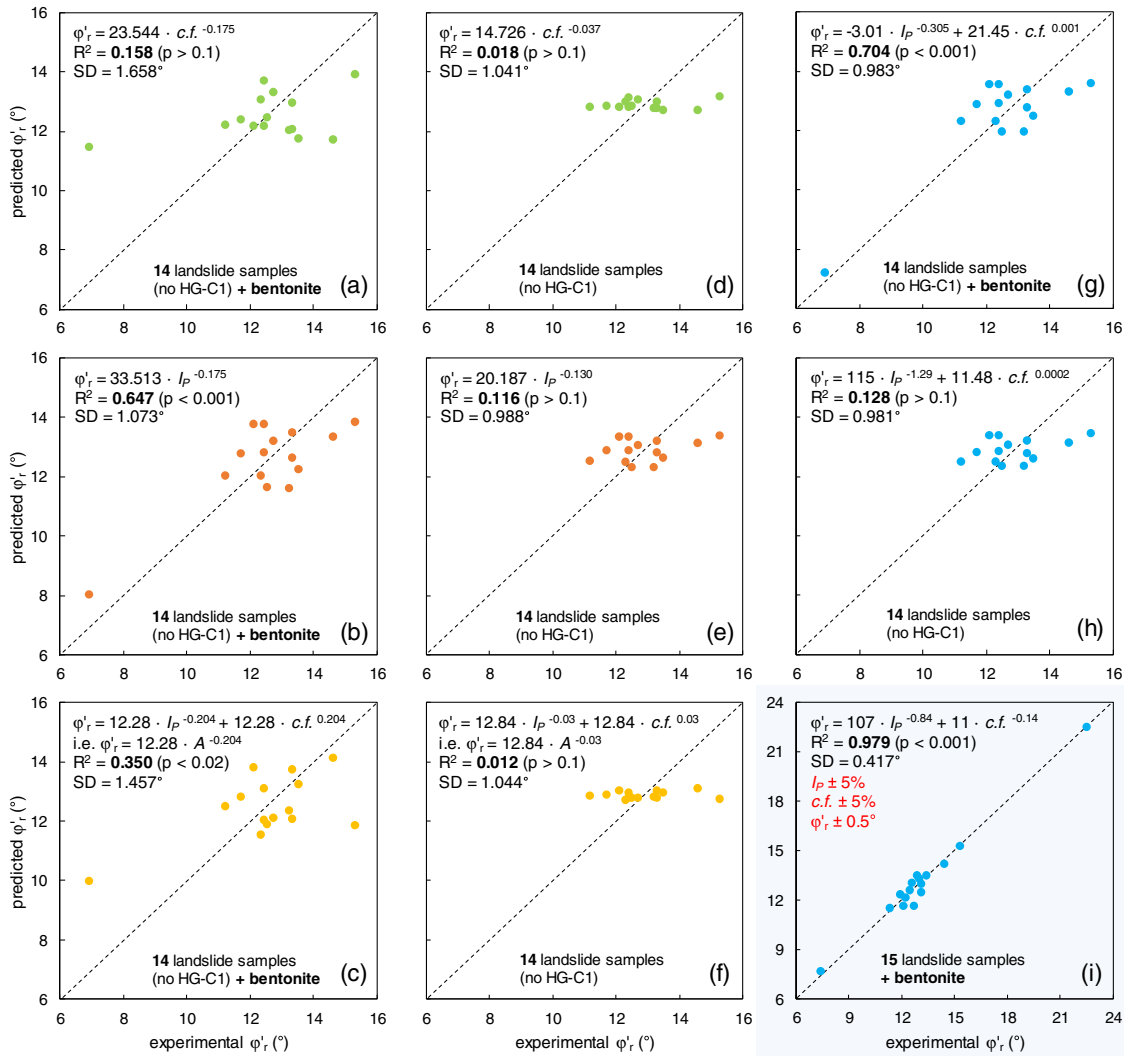


**Fig. 8** Optimised models to estimate  $\phi'_r$  from index properties: power function of  $c.f.$  (a, d); power function of  $I_P$  (b, e); power function of  $A = I_P/c.f.$  (c, f); linear combination of power functions of  $c.f.$  and  $I_P$  (g, h, i). Note that the sample of bentonite has been excluded from (d, e, f, h). In i, uncertainties of  $\pm 0.5^\circ$  on  $\phi'_r$ ,  $\pm 5\%$  on  $I_P$  and  $\pm 5\%$  on  $c.f.$  were permitted during model training. SD indicates the standard deviation between experimental and predicted values of  $\phi'_r$

while  $A$  performs worse ( $R^2 = 0.350$ ,  $p < 0.02$ ; Fig. 8c), and the correlation with  $c.f.$  is insignificant ( $R^2 = 0.158$ ,  $p > 0.1$ ; Fig. 8a). In Fig. 8g, an optimised correlation has been found between  $\phi'_r$  and both  $c.f.$  and  $I_P$  in the form of a linear combination of two power laws, one depending on  $c.f.$  and one on  $I_P$ . This correlation performs only slightly better than that with  $I_P$  alone ( $R^2 = 0.704$ ,  $p < 0.001$ ), despite the non-negligible correlation between  $c.f.$  and  $\phi'_r$  (Fig. 8a). This is due to  $I_P$  being itself correlated with  $c.f.$  (e.g.  $\ln I_P = 0.0122c.f. + 2.9635$ ,  $R^2 = 0.36$ ,  $p < 0.02$  in our dataset), which is a feature known in the literature.

In a second set of analyses, the sensitivity of the optimised correlations to the input dataset is explored by excluding the values relative to the bentonite. This sample, being significantly different from the others, is shown to affect the optimised solution the most. Interestingly, as shown in Fig. 8d, e, f and h, all optimised models perform poorly, indicating

that the variability of  $\phi'_r$  in this reduced data set (14 landslide soil samples) cannot be explained by the variability of index properties. The model accounting for both  $I_P$  and  $c.f.$  (Fig. 8h) also performs poorly ( $R^2 = 0.128$ ,  $p > 0.1$ ).

## Discussion

### Sensitivity of correlations

Experimental data, even when obtained through duly-performed, standardised laboratory tests, are still affected by uncertainties of stochastic nature. Taking such uncertainties into account is fundamental especially in analyses that are sensitive to small variations in the input parameters, such as hazard assessments, landslide volume calculations, or slope stability analyses in conditions very close to instability (e.g. Fan et al. 2018, 2019; Scaringi et al. 2018a). With Fig. 8i, we wish to show to what (large) extent accounting for (small but reasonable) uncertainties in the input data set can affect the result of a

simple empirical correlation (cf. Fig. 8h). To this purpose, an uncertainty of  $\pm 5\%$  for  $c.f.$  has been introduced, which might actually be lower than what declared by laboratories that perform standardised evaluations of grain size distributions (6–8%). Reasonable uncertainties of  $\pm 5\%$  for  $I_p$  and  $\pm 0.5^\circ$  for  $\phi'_r$  have also been introduced. As an additional constraint, it has been assumed that the experimental values were not affected by systematic errors, i.e. by consistently positive or negative errors. To account for this assumption, it has been imposed (arbitrarily) that the average of the residuals must be less than  $\pm 10\%$  of the uncertainty range, and the standard deviation must be less than  $\pm 60\%$  of the uncertainty range. In other words, the evolutionary model has been allowed to modify the input data within the given uncertainty ranges, but with the conditions that these modifications would not modify the averages and distributions of the data significantly. Figure 8h shows that the empirical correlation is very sensitive even to small and constrained uncertainties. In fact, the optimised solution, found across the entire data set (15 landslide samples + bentonite) features a very high coefficient of determination ( $R^2 = 0.979$ ,  $p < 0.001$ ), with predicted  $\phi'_r$  deviating from the experimental ones by less than  $1^\circ$  at a confidence level of 95% ( $SD = 0.417^\circ$ ). It is worth noting that, by investigating the modifications made by the evolutionary solver while seeking the optimised solution, we find that the values relative to HG-C1 have been changed only slightly (i.e. the solver took the experimental data as good): the best fit was found by changing  $c.f.$  by only 1%, and  $I_p$  and  $\phi'_r$  by 0.5%.

#### Choice of shear device and sample size

Applying an empirical correlation calibrated on residual strength measurements in a direct shear device, rather than in a ring shear apparatus, is in principle a source of bias, and comparing empirical and experimental data obtained with different apparatuses might produce additional uncertainty. Various authors have reported that the residual shear strength evaluated in a direct shear apparatus can be significantly higher than that obtained in a ring shear (e.g. Bishop et al. 1971; Hawkins and Privett 1985). Especially under low normal stress, a difference of up to  $7^\circ$  in residual friction angle has been evaluated (Hutchinson et al. 1980), with the value obtained in the ring shear more closely resembling the strength available/mobilised in situ in shear zones after large strains.

However, various works also report results obtained with ring and direct shear devices that are practically coincident. It can be hypothesised, in this case, that the effect of other uncertainties overcomes the control exerted by the different boundary/testing conditions imposed by the devices. Results in this sense are reported in Scaringi et al. (2013), Scaringi (2016) and Scaringi and Di Maio (2016). A more detailed comparison is given in Hawkins and Privett (1985). Mesri and Shahien (2003), Stark et al. (2005) and Mesri and Huvaj-Sarhan (2012) also agree that the residual shear strength evaluated in direct shear tests can represent the residual shear strength *in situ* well, even though the use of a ring shear device remains preferable (cf. also Meehan et al. 2007). In all the abovementioned cases, however, key to this conclusion seems a careful execution of the direct shear test, to ensure that the shear surface remained flat and located within the gap between the two halves of the shear box. This is done by pre-cutting and even polishing the specimens after consolidation, for instance through

a thin blade or wire. The operation might also be repeated during the shearing phase if irregularities in the shear-displacement plot are noticed (e.g. due to material extrusion, or significant secondary compression), and after each new consolidation phase.

Sample size is another factor influencing the experimental determination of a soil's shear strength. However, evaluating the extent to which different sample sizes may add uncertainty to empirical correlations is not a straightforward task. In principle, using the same set of materials, carefully homogenised, a large number of direct shear specimens with different cross sections could be prepared (e.g. using a  $60 \times 60$  mm square box, a  $100 \times 100$  mm square box, a 50-mm-diameter circular box, etc.), and the same could be done for ring shear specimens. Moreover, the specimen's height could be changed (e.g. to investigate possible roles of lateral friction during shearing) and, in the case of direct shear, also the effect of the amount of shear displacement in each shear cycle could be investigated. In fact, various studies have compared shear strength values determined on samples of different sizes. For instance, Hawkins and Privett (1985), while investigating a clay soil ( $\phi'_r \sim 6^\circ$ ), found that a larger shear box ( $100 \times 100$  mm) provided values of residual shear strength close to those obtained in a Bromhead-type (Bromhead 1979) ring shear device, while a smaller box ( $60 \times 60$  mm) provided significantly higher values. The smaller box, according to the authors, is more prone to frictional and other intrinsic problems. This also translates in the large variability of  $\tau_r$  (greater than  $\pm 25\%$ ) that they observed upon testing the same material in the same stress range ( $\sigma_v = 50 - 600$  kPa) using two distinct boxes of the same size ( $60 \times 60$  mm). On the other hand, it is worth noting that Thermann et al. (2006), investigating the strength of glacial tills in direct shear boxes, found no significant effect of sample size (71.4 mm or 94.4 mm in diameter) when testing  $\sigma_v = 100 - 500$  kPa. However, their result refers to an unsaturated non-clay soil, for which the peak strength was the object of evaluation. Palmeira and Milligan (1989) also did not report significant sample size effects (from  $60 \times 60$  mm to  $1 \times 1$  m) on the evaluated strength while testing a medium sand. A similar result was obtained by Garga (1988) on a basaltic residual soil using direct shear boxes ( $101.6 \times 101.6$  mm or 63.5 mm in diameter), who evaluated differences in friction angle less than  $1^\circ$ .

When comparing our experimental results and correlations with those from the literature, it should be noted that we and Stark and Hussain (2013) utilised a Bromhead-type ring shear apparatus with inner diameter of 70 mm, outer diameter of 100 mm, and sample height of 5 mm. Therefore, our results in terms of  $\phi'_r$  should be comparable straightforwardly. Xu et al. (2018) used a Bishop-type ring shear apparatus with larger sample size (thus in principle less uncertainty), namely with inner diameter of 100 mm, outer diameter of 150 mm, and height of 20 mm. Kanji (1974) used a  $60 \times 60$  mm direct shear box (cf. Kanji 1973; thus in principle more uncertainty than in our case, and possible overestimation of the strength). Kenney (1959) used a triaxial apparatus, with samples of 1.5" in diameter ( $\sim 38$  mm) and 3.5" in height ( $\sim 76$  mm) (cf. also Kenney and Watson 1961), which are of the same size as our triaxial samples. On the other hand, the dataset used by Muir Wood (1990) included results from different sources, possibly obtained on samples of various sizes.

Quantifying data dispersion and uncertainties related to correlations from the literature would require access and re-analysis of the complete datasets, as well as detailed information on the testing procedures. This is unfortunately, beyond our reach. However, the reader must be warned that, when comparing results across various correlations and experimental results (see “Comparison with results of back analyses” section, below) further, non-quantified, uncertainties related to choices in the experimental setups, as well as to the characteristics of the correlations (e.g. standard deviation, significance level), should be added. In developing new correlations, it is advised to make a careful choice of the testing procedure to constrain errors and uncertainties as much as possible, to keep the procedure consistent throughout the dataset, and to provide detailed statistics on the obtained correlations, including a sensitivity analysis for uncertainties not constrained in the testing phase (see Figs. 7 and 8, “Sensitivity of correlations” section).

### Effect of shearing rate

The rate of shearing is one experimental setting that may affect the evaluation of the shear strength, which has received specific attention in the literature (e.g. Tika et al. 1996; Scaringi and Di Maio 2016) and deserves a dedicated discussion. We conducted some ring shear tests under various rates of displacement in the range 0.018–44.5 mm/min (i.e. 2.6 cm/day–2.7 m/h), with the aim of assessing the possible effect of the rate on the residual shear strength. The range we investigated covers the full extent of rates allowed by the experimental apparatus, as well as the maximum rate exhibited by the Dobrovický landslide (1 m/h); it corresponds to *slow*, *moderate* and *rapid* landslide movements in the classification of Cruden and Varnes (1996). We tested IG 214 ( $I_p = 44.3\%$ ) and IND 204 ( $I_p = 26.9\%$ ) and, for comparison, also a sample of commercial quartz sand from *Streleč* quarry (Czech Republic, commercial name STJ25), and a commercial Ca-Mg bentonite from *Černý vrch* deposit (Keramost a.s., Czech Republic,  $I_p = 166.1\%$ ; Table 1). All tests were performed under  $\sigma_v = 50\text{ kPa}$ . Here, we used total rather than effective stresses because drained conditions cannot be assured at all rates, and we could not measure pore water pressures during the tests. Figure 9 shows the ratio between  $\tau_r$  evaluated at a given rate and  $\tau_r$  obtained at the lowest rate ( $v = 0.018\text{ mm/min}$ ). In the figure, we compare the experimental data obtained in this work to results of tests on clayey soils, pure clays and sands from the literature.

We did not observe significant rate effects, i.e.  $(\tau_r - \tau_{r,v=0.018\text{ mm/min}})/\tau_r < 10\%$ , for  $v \leq 1\text{ mm/min}$ , consistently with results on clays and sands from Scaringi and Di Maio (2016). At higher rates, IG 214 exhibited a positive rate effect, gaining up to 15% of residual shear strength ( $\sim 2^\circ$  of friction angle) over an increase of rate of three orders of magnitude. It can be hypothesised that a strength increase of the same amount might have occurred during the landslide runout, and could have effectively limited the maximum landslide velocity, and thus its destructive potential. On the other hand, IND 204 did not show significant rate effects under the investigated rates.

For comparison, we observed the largest positive rate effect on the bentonite, with a strength increase of  $\sim 20\%$  across the investigated rates. The result is very close to what observed by Scaringi and Di Maio (2016) on a Na-montmorillonite. It is worth noting that IG 214 has  $c. f. = 46\%$  and  $A = 1.0$  (which is higher than the

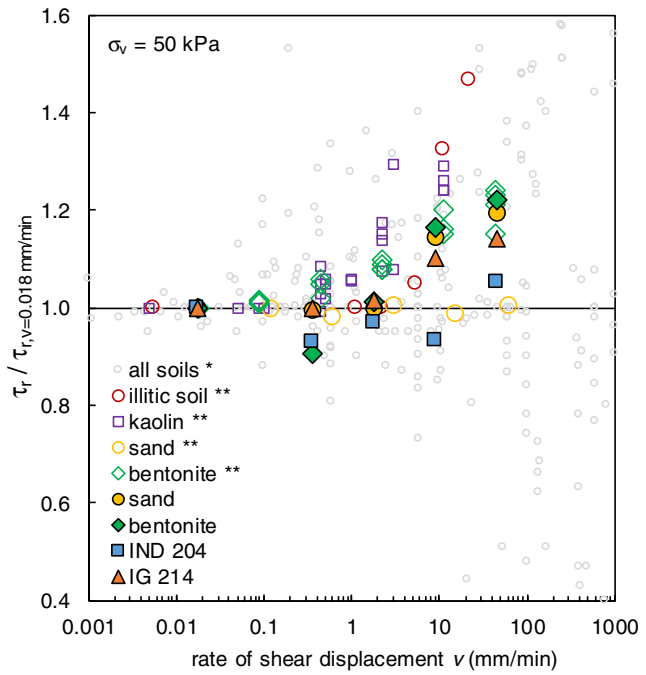


**Fig. 9** Residual shear strength  $\tau_r$  against the rate of displacement  $v$ , normalised by  $\tau_r$  evaluated at  $v = 0.018\text{ mm/min}$ . Solid markers indicate the original data, obtained under  $\sigma_v = 50\text{ kPa}$ . Hollow markers indicate data from the literature, evaluated under  $\sigma_v = 50 - 500\text{ kPa}$ ; (\*) collection of data from Tika et al. (1996), Scaringi and Di Maio (2016), Hu et al. (2017) and Scaringi et al. (2018b); (\*\*) data from Scaringi and Di Maio (2016), where the illitic soil comes from *Costa della Gaveta* landslide (Italy), the bentonite is mostly made of Na-montmorillonite, the kaolin is of *Speswhite* quality, and the sand is a quartz medium sand

activity of pure illite; Skempton 1953). On the other hand, IND 204 has  $c. f. = 54\%$  and  $A = 0.5$  (which is close to that of kaolinite; Skempton 1953). Illitic soils, kaolins and bentonites have all shown significant positive rate effects (e.g. Scaringi and Di Maio 2016). Conversely, soils containing a small proportion of clay minerals often show negative rate effects (e.g. Scaringi et al. 2018b, c; Tika et al. 1996; Hu et al. 2017, 2018; Scaringi and Di Maio 2016). Therefore, explaining the inconsistent result of IND 204 would demand a mineralogical investigation.

### Effect of clay-size fraction

Skempton (1964) observed a large scatter in the experimental data utilised to build a correlation

between  $c. f.$  and  $\phi'_r$ , which causes it to perform very poorly if used to make predictions. The scatter can be attributed to the difference between clay fractions in granulometric and mineralogic senses, as well as in significant differences in strength across clay minerals of different nature (e.g. Kenney 1967; Scaringi and Di Maio 2016). We verified this in our dataset using four materials, namely IND 204 ( $I_p = 26.9\%$ ), IG 214 ( $I_p = 44.3\%$ ), the commercial bentonite ( $I_p = 166.1\%$ ) and the commercial sand (cf. Table 1). By sieving and sedimentation, the clay-size fractions of the two landslide soil samples were separated from the coarser fractions. Then, mixtures of landslide soils or bentonite with sand were prepared and specimens were reconstituted and submitted to ring shear tests under  $\sigma'_v = 30, 50, 70, 120\text{ kPa}$  to evaluate  $\phi'_r$ . The results are

summarised in Fig. 10, where  $\phi'_r$  values of all mixtures, as well as those of the landslide soil samples, are plotted against their  $c.f.$  and compared to upper and lower bounds from the literature (Skempton 1964).

The correlation between  $c.f.$  and  $\phi'_r$  is markedly non-linear and shows a sigmoidal shape. Within the range reported in the literature, experimental points close to the lower bound indicate soils containing very active clay minerals (e.g. montmorillonite), for which a small percentage of clay-size particles is sufficient to produce low values of  $\phi'_r$ , that are closer to values typical of a pure clay than to those of a pure sand. Vice versa, points close to the upper bound suggest that the soil contains clays with low activity (e.g. kaolinite), which needs to be present in large proportion to affect the  $\phi'_r$  significantly. Consistently, the results relative to sand-bentonite mixtures plot close to the lower bound (Fig. 10), showing that a  $c.f.=50\%$  is sufficient to obtain values of  $\phi'_r$  very close to those of pure montmorillonite (e.g. Scaringi and Di Maio 2016). Results relative to sample IG 214 are similar, suggesting that also this soil contains a significant proportion of smectite-group minerals. The different nature of sample IND 204 also stands out from the figure. The points of all landslide soil samples (not mixed with sand) all plot close to, or even below Skempton's (1964) lower bound, possibly because of a small but very active clay component. In the figure,

the empirical correlations calibrated on data from these soil samples through optimised models (Fig. 8a and d) are also reported for comparison. It is clear that the peculiarities of the calibration set, which moreover only covers a limited range of  $c.f.$  and  $\phi'_r$ , result in correlations that are significantly different from others from the literature (Skempton 1964), and are hardly applicable in other contexts or to different soils.

In order to confirm what the results in Fig. 10 suggest in terms of soil mineralogy, the composition of the samples was quantified by conventional powder X-ray diffraction (P-XRD) in the Laboratory of the Czech Geological Survey. The results of the analyses (Table 3) confirm the high percentage of smectite-group minerals in the commercial bentonite and in the landslide soil sample IG 214. As for sample IND 204, they show that, despite the high clay-size fraction ( $c.f.=54\%$ ), the material is poor of clay minerals which, moreover, belong to low-active types (kaolinite and mica). Part of the clay-size fraction is constituted by non-clay minerals (calcite and quartz powder), which explains the low activity (cf. Table 1) and might also explain the inconsistent results shown in “Effect of shearing rate” section relative to the shear rate dependence of  $\phi'_r$ .

#### Comparison with results of back analyses

In order to summarise the results obtained in this work, we carried out the following analysis (Fig. 11): the probability density distributions of the experimentally determined values of  $\phi'_{cr}$  and  $\phi'_r$  were obtained, as well as the distributions of the values of the same parameters estimated from various empirical correlations with  $I_p$  from the literature, or using correlations calibrated in this work (cf. “Empirical estimates of strength parameters” section). Note that, in doing so, the uncertainties intrinsic to the correlations (data dispersion, tested materials, effects of the shear device and test conditions) were not taken into account (cf. discussion in “Choice of shear device and sample size” section). It is expected that including them would further increase the dispersion of the probability density distributions, thereby decreasing the significance of our conclusions, and even change their modal value to some extent (e.g. in case of systematic under- or over-estimation of the strength parameter). It should be noted in this sense, for instance, that Kanji's (1974) correlation was obtained on results of direct shear tests, while here it is applied on results of ring shear tests.

The probability densities in Fig. 11 were calculated—under the assumption that the determined/estimated strength parameters are normally distributed—using only the values of  $I_p$ ,  $c.f.$ ,  $\phi'_{cr}$  and  $\phi'_r$  obtained from soil samples extracted from the shear zone of the Dobkovičky landslide (10 samples, cf. Table 1). In this way, the distributions could be compared with values of mobilised friction angle calculated by Stemberk et al. (2016) through back analysis. The authors carried out both 2D and 3D analyses, using a Mohr-Coulomb failure criterion and the method of strength reduction in Plaxis 3D (Plaxis BV), or a set of methods of slices in Slope/W (GeoSlope Intl. Ltd.). The analyses were carried out with different hydraulic boundaries, in short-term and long-term conditions, which required both unsaturated and saturated strength concepts to be considered (cf. “The shear strength

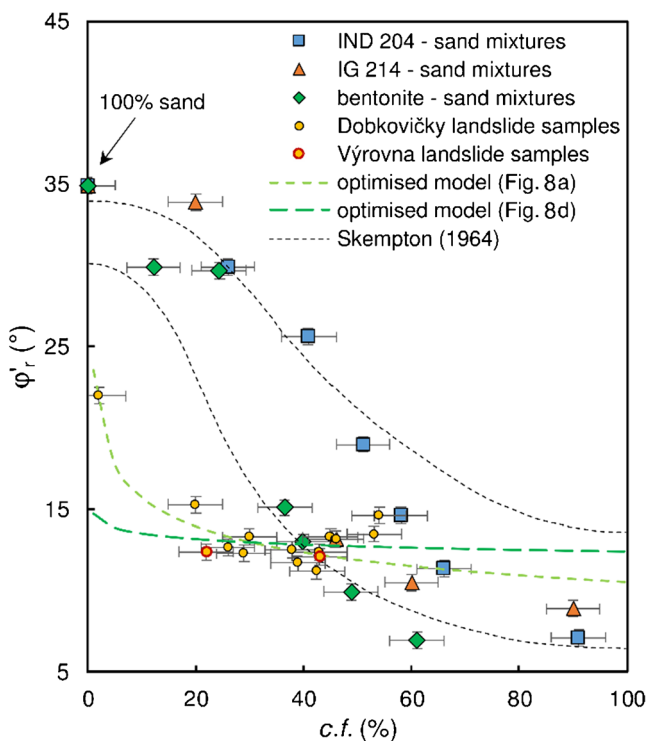
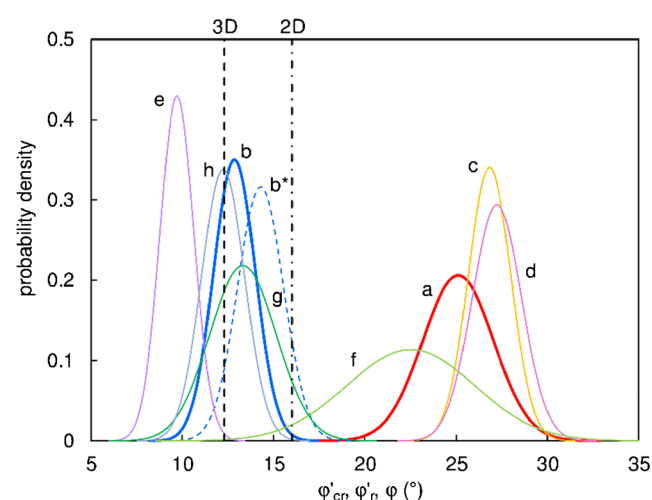


**Fig. 10** Correlation between clay fraction ( $c.f.$ ) and residual friction angle ( $\phi'_r$ ) of soil samples from Dobkovičky and Výrovna landslides, and of mixtures of some clayey soils with sand (cf. Table 1 for their characterisation). Upper and lower bounds are from Skempton (1964); error bars are  $\pm 0.5^\circ$  for  $\phi'_r$  and  $\pm 5\%$  for  $c.f.$ ; dashed lines are the correlations obtained through the optimised models shown in Fig. 8a and d

**Table 3** Mineralogy of samples IND 204, IG 214, commercial bentonite, and sand

| Sample    | Calcite | Quartz | Kaolinite | Pyroxene | Mica | Goethite | Anatase | Smectite |
|-----------|---------|--------|-----------|----------|------|----------|---------|----------|
| IND 204   | 68      | 17     | 4.5       |          | 10.5 |          |         |          |
| IG 214    | 5       | 18.5   |           | 6        | 8    |          |         | 62.5     |
| Bentonite | 2       | 9.5    |           |          |      | 1.5      | 1       | 86       |
| Sand      |         | 99.3   |           |          |      |          |         |          |

for stability analyses” section). The most burdensome case, with shallow groundwater table and a fully saturated shear zone, was deemed representative of the condition at the time of failure. In such condition, a mobilised effective friction angle of  $\phi = 12.3^\circ$  was evaluated in the 3D analysis, and of  $\phi = 16^\circ$  in the 2D analysis (uncertainties were not specified). The difference between 2D and 3D results was attributed by the authors to the geometry of the landslide body, for which a 2D approximation was deemed inappropriate. Detailed descriptions of the analysis cases, the model geometry and constraints, and the subsurface hydraulic and geotechnical models, can be found in Stemberk et al. (2016), or obtained from the authors upon request.



- a  $\phi'_c$  determined experimentally (own data, Tab. 1)
- b  $\phi'_r$  determined experimentally (own data, Tab. 1)
- - - b\*  $\phi'_r$  estimated at the maximum landslide velocity (1 m/h; Fig. 9)
- c  $\phi'_c$  estimated from  $I_p$  (Kernrey 1959, Fig. 6)
- d  $\phi'_c$  estimated from  $I_p$  (Muir Wood 1990, Fig. 6)
- e  $\phi'_r$  estimated from  $I_p$  (Kanji 1974, Fig. 6)
- f  $\phi'_r$  estimated from  $I_p$  (Xu et al. 2018, Fig. 6)
- g  $\phi'_r$  estimated from  $\phi'_c$  (own data, Fig. 5b)
- h  $\phi'_r$  estimated from  $I_p$  and c.f. (own data, Fig. 8i)
- - - φ mobilised (2D back analysis, Stemberk et al. 2016)
- - - φ mobilised (3D back analysis, Stemberk et al. 2016)

**Fig. 11** Comparison of statistical distributions of strength parameters ( $\phi'_c$ ,  $\phi'_r$ ), determined experimentally or evaluated by empirical correlations with index properties, with back-calculated values of the mobilised friction angle by 2D or 3D stability analyses (Stemberk et al. 2016). The probability density distributions were obtained under the assumption that the determined/estimated friction angles follow a normal distribution

Figure 11 shows that the result of the 3D analysis is consistent with the distribution of  $\phi'_r$  obtained from the experimental data (curve b), while the result of the 2D analysis is significantly different. We can calculate that the probability of  $\phi'_r$  being within  $\pm 10\%$  from the value obtained by the 3D analysis is 66%, which becomes over 85% if the range is extended to  $\pm 15\%$ . If the effect of shearing rate on  $\phi'_r$  is accounted for (curve b\*; cf. also “Effect of shearing rate” section and Fig. 9), we can infer that when the landslide reached its maximum velocity (1 m/h), the safety factor calculated in the 3D analysis had become larger than 1 ( $p < 0.05$ ). This is consistent with a feedback mechanism of the rate of displacement on the mobilised shear strength, which might have prevented further acceleration of the landslide body.

The distribution of  $\phi'_c$  values (curve a) lies completely to the right ( $p < 0.001$ ) of the results of both 2D and 3D analyses, which would exclude  $\phi'_c$  from being the relevant strength parameter of the landslide of June 2013. If estimations of  $\phi'_c$  and  $\phi'_r$  by empirical correlations from the literature are used, the picture becomes more confused. While  $\phi'_c$  remains excluded because very high values are obtained (curves c and d), contrasting results are obtained for  $\phi'_r$ . In fact, if Kanji’s (1974) correlation is used, one must conclude ( $p < 0.003$ ) that the mobilised strength is most certainly higher than  $\phi'_r$ , while if Xu et al.’s (2018) correlation is used, the conclusion ( $p < 0.002$ ) is that the mobilised strength is lower than  $\phi'_r$ , which is absurd unless the evaluation of  $I_p$  suffered from a (very) large systematic error.

Figure 11 also shows the distributions of  $\phi'_r$  obtained using some of the correlations calibrated on samples from the Dobkovický landslides and its surroundings, the Výrovna landslide, and the commercial bentonite (cf. “Empirical estimates of strength parameters” section). Note that the use of these correlations for predicting the strength parameter is inappropriate in this context, as a subset of the calibration data set is being used as an input. The results (curves g and h), which are obviously consistent with those of the experimentally-determined values (curve b) have been included in the figure for comparison only. Nevertheless, they highlight that the evaluation of  $\phi'_r$  from  $\phi'_c$  is affected by a larger dispersion (curve g; cf. also Fig. 5b) than that from  $I_p$  and c. f. (curve h; cf. also Fig. 8i), which was obtained through an optimised model. This is also reflected by the fact that the probability of  $\phi'_r$  being within  $\pm 10\%$  from the value obtained by the 3D back analysis is less than 44% for curve g, while it is about 70% for curve h.

## Conclusions and recommendations

Accurate evaluations of the shear strength mobilised by landslides are critical for assessing the stability of soil slopes and landslide bodies, as well as for predicting their post-failure behaviour. While direct determinations by laboratory shear tests are always preferred, preliminary evaluations by empirical correlations with the soil index properties can be useful in the engineering practice. By verifying the performance of selected empirical correlations from the literature against values of  $\phi'_{cr}$  and  $\phi'_r$  measured in the laboratory, we found systematic deviations that might originate both from a biased set of data used to build the correlations (not representative of the soil type under investigation, or not populous enough), and from uncertainties in the determination of the index and strength parameters (including, for the latter, the choice of the shear device, the sample size, and the rate of shearing). However, we also pointed out that estimates of  $\phi'_{cr}$  are close enough to the experimental values and might be used in preliminary stability analyses. Conversely, estimates of  $\phi'_r$  showed large deviations, as anticipated on the basis of theoretical considerations, which make their use in stability analyses less confident, if not unfeasible.

Using sets of correlations calibrated on our experimental data we observed that, in general, individual index properties can only explain a (minor) part of the observed variability in shear strength. The best predictor for both  $\phi'_{cr}$  and  $\phi'_r$  was the plasticity index, consistently with what known from the literature, while the clay-size fraction was not informative in our case. Furthermore, the predicted values showed a significant scatter, which could be partly explained by taking the mineralogy of the clay component into account, whereas the remaining variability could be attributed to reasonable uncertainties in the evaluation of index properties and strength parameters. This finding implies that even small uncertainties, especially in relatively homogeneous sets of soil samples, can override the predictive capability of the index properties. The information on mineralogy is generally not obtained in routine experimentations, while that on the uncertainty is provided by the laboratory and/or by the standard testing protocols, but is often neglected in practice.

In conclusion, we recommend to use caution in proposing empirical correlations based on limited data sets, on data obtained from different shear devices, or on samples of multiple sizes, and in applying such correlations to different types of soil or effective stress ranges. We also remind that experimental data must always be accompanied by their uncertainties, or reasonable estimations must be made in case they are not provided. As for the applicability of the empirical correlations, we suggest to rely on them—provided that they have proven robust enough and perform reasonably well for the type of soil under investigation—only as first-order approximations of the strength parameters in preliminary analyses or in regional assessments. In specific analyses (individual slopes or portions of slopes, individual landslide bodies), we feel that results from properly-performed shear tests are always required for reliable stability analyses. Furthermore, the variability in soil properties in the domain of interest, as well as its hydraulic conditions and possible variable saturation, must not be neglected. Finally, for more

advanced simulations and predictions of stresses and strains in the whole domain, more specific sets of parameters must be determined anyway, which may include hydraulic and elastic properties, as well as time-dependent and shear rate-dependent features.

## Acknowledgements

The authors wish to thank SG Geotechnika, Gematest, and the laboratory of the Czech Geological Survey for providing part of the experimental data. The authors are grateful to the editor Prof. Anthony Leung, and to Dr. Anil Yildiz, and one anonymous referee for their helpful comments which contributed greatly to the current form of this work.

## Funding information

This study is financially supported by the Czech Science Foundation (GAČR) under the Project 17-21903S. J. Roháč is supported by the Project 1488217 of the Grant Agency of Charles University (GAUK). G. Scaringi is financially supported by the Fund for International Mobility of Researchers at Charles University (project no. CZ.02.2.69/0.0/0.0/16\_027/0008495, key activity 1-PřF-GEOMOBIL).

## References

Ameratunga J, Sivakugan N, Das BM (2016) Correlations of soil and rock properties in geotechnical engineering. Springer, India, 228 pp. <https://doi.org/10.1007/978-81-322-2629-1>

ASTM (2011) D2487-11. Standard Practice for Classification of Soils for Engineering Purposes (Unified Soil Classification System). ASTM International, West Conshohocken

Baker KR (2011) Solving sequencing problems in spreadsheets. *Int J Plan Sched* 1:3–18

Baker KR, Camm JD (2005) On the use of integer programming versus evolutionary solver in spreadsheet optimization. *INFORMS Trans Educ* 5:1–7

Bishop AW, Green GE, Garga VK, Andresen A, Brown JD (1971) A new ring shear apparatus and its application to the measurement of residual strength. *Géotechnique* 21(4):273–328

Bjerrum L, Simons NE (1960) Comparison of Shear Strength Characteristics of Normally Consolidated Clays, NGI-Publ

Bromhead EN (1979) A simple ring shear apparatus. *Ground Eng* 12(5)

Brooker EW, Ireland HO (1965) Earth pressures at rest related to stress history. *Can Geotech J* 2(1):1–15

Brooks RH, Corey AT (1964) Hydraulic properties of porous media. *Hydrology paper No3*, Colorado State University

Burland JB (1990) On the compressibility and shear strength of natural clays. *Géotechnique* 40:329–378. <https://doi.org/10.1680/geot.1990.40.3.329>

Cajz V (2000) Proposal of lithostratigraphy for the České středohoří Mts. volcanics. *Bull Czech Geol Surv* 75:7–16

Cruden DM, Varnes DJ (1996) Landslide types and processes, special report, Transportation Research Board, National Academy of Sciences, 247:36–75

D'Onza F, Gallipoli D, Wheeler S, Casini F, Vaunat J, Khalili N, Laloui L, Mancuso C, Mašín D, Nuth M, Pereira JM, Vassallo R (2011) Benchmark of constitutive models for unsaturated soils. *Géotechnique* 61(4):283–302

De La Fuente S, Cuadros J, Linares J (2002) Early stages of volcanic tuff alteration in hydrothermal experiments: Formation of mixed-layer illite-smectite. *Clay Clay Miner* 50:578–590

Di Maio C, Fenelli GB (1994) Residual strength of kaolin and bentonite: the influence of their constituent pore fluid. *Géotechnique* 44:217–226. <https://doi.org/10.1680/geot.1994.44.2.217>

Di Maio C, Santoli L, Schiavone P (2004) Volume change behaviour of clays: the influence of mineral composition, pore fluid composition and stress state. *Mech Mater* 36:435–451

Di Maio C, Scaringi G, Vassallo R (2015) Residual strength and creep behaviour on the slip surface of specimens of a landslide in marine origin clay shales: influence of pore fluid composition. *Landslides* 12:657–667. <https://doi.org/10.1007/s10346-014-0511-z>

Fan X, Domènec G, Scaringi G, Huang R, Xu Q, Hales TC, Dai L, Yang Q, Francis O (2018) Spatio-temporal evolution of mass wasting after the 2008 Mw 7.9 Wenchuan

Earthquake revealed by a detailed multi-temporal inventory. *Landslides*. <https://doi.org/10.1007/s10346-018-1054-5>

Fan X, Scaringi G, Domènec G, Yang F, Guo X, Dai L, He C, Xu Q, Huang R (2019) Two multi-temporal datasets that track the enhanced landsliding after the 2008 Wenchuan earthquake. *Earth Syst Sci Data* 11:35–55. <https://doi.org/10.5194/essd-11-35-2019>

Gamez JA, Stark TD (2014) Fully softened shear strength at low stresses for levee and embankment design. *J Geotech Geoenvir* 140(9):06014010

Garga VK (1988) Effect of sample size on shear strength of basaltic residual soils. *Can Geotech J* 25(3):478–487

Gudehus G (2011) Physical soil mechanics. Springer-Verlag, Berlin Heidelberg 839 pp

Hawkins AB, Privett KD (1985) Measurement and use of residual shear strength of cohesive soils. *Ground Engineering*. 1985;18(8)

Hu W, Xu Q, Wang G, Scaringi G, McSaveney M, Hicher P-Y (2017) Shear Resistance Variations in Experimentally Sheared Mudstone Granules: A Possible Shear-Thinning and Thixotropic Mechanism. *Geophys Res Lett* 44:11,040–11,050. <https://doi.org/10.1002/2017GL075261>

Hu W, Scaringi G, Xu Q, Van Asch TWJ, Huang R, Han W (2018) Suction and rate-dependent behaviour of a shear-zone soil from a landslide in a gently-inclined mudstone-sandstone sequence in the Sichuan basin, China. *Eng Geol* 237:1–11. <https://doi.org/10.1016/j.enggeo.2018.02.005>

Hungr O, Leroueil S, Picarelli L (2014) The Varnes classification of landslide types, an update. *Landslides* 11:167–194. <https://doi.org/10.1007/s10346-013-0436-y>

Hutchinson NJ, Bromhead EB, Lupini JF (1980) Additional observations on the Falkstone Warren Landslides. *Q J Eng Geol* 13:1–31

Hvorslev MJ (1937) Über die Festigkeitseigenschaften gestorter bindiger Boden. *Ingénierividskabelige Skr Dan Naturvidenskabelige Samf Diss*

ISO 17892-12 (2004) Geotechnical investigation and testing – laboratory testing of soil – Part 12: Determination of Atterberg limits

ISO 17892-9 (2004) Geotechnical investigation and testing – laboratory testing of soil – Part 9: Consolidated triaxial compression tests of water-saturated soil

Kanji MA (1973) Resistência ao cisalhamento de contactos solo-rocha. Doctoral Thesis, São Paulo, Brazil. <https://doi.org/10.11606/T.44.2016.tde-07072016-085900>

Kanji MA (1974) The relationship between drained friction angles and Atterberg limits of natural soils. *Géotechnique* 24:671–674. <https://doi.org/10.1680/geot.1974.24.4.671>

Kaya A (2010) Revisiting correlations between index properties and residual friction angle of natural soils using artificial neural networks. *Geomechanics and Geoengineering: An International Journal* 5(2):109–116. <https://doi.org/10.1080/1748602903497423>

Kaya A, Kwong JPK (2007) Evaluation of common practice empirical procedures for residual friction angle of soils: Hawaiian amorphous material rich colluvium soil case study. *Eng Geol* 92(1–2):49–58

Kenney TC (1959) Discussion of "Geotechnical Properties of Glacial Lake Clays" by T. H. Wu, *Journal of the Soil Mechanics and Foundations Division*. ASCE 85(SM3, Part 1):67–79

Kenney TC (1967) The influence of mineral composition on the residual strength of natural soils. In: Proc. Geotechnical conference, Oslo, pp 123–129

Kenney TC, Watson GH (1961) Multiple-stage triaxial test for determining  $c'$  and  $\phi'$  of saturated soils. Technical Memorandum, Division of Building Research, National Research Council Canada 72-2:1–5

Khalili N, Khabbaz MH (1998) A unique relationship for  $\chi$  for the determination of the shear strength of unsaturated soils. *Géotechnique* 48(5):681–688

Ladd CC, Foott R, Ishihara K, Schlosser F, Poulos HG (1977) Stress-deformation and strength characteristics. Proc. 9th. Int. conf. soil mech. and found. Eng. pp. 421–494

Leroueil S (2001) Natural slopes and cuts: movement and failure mechanisms. *Géotechnique* 51:197–243

Lu N, Likos WJ (2004) Unsaturated soil mechanics. John Wiley & Sons 556pp

Lupini JF, Skinner AE, Vaughan PR (1981) The drained residual strength of cohesive soils. *Géotechnique* 31:181–213

Mašín D (2010) Predicting the dependency of a degree of saturation on void ratio and suction using effective stress principle for unsaturated soils. *International Journal for Numerical and Analytical Methods in Geomechanics* 34, No. 1, 73–90

Mašín D (2012) Asymptotic behaviour of granular materials. *Granular Matter* 14(6):759–774

Meehan CL, Brandon TL, Duncan JM (2007) Measuring drained residual strengths in the Bromhead ring shear. *Geotech Test J* 30(6):466–473

Mesri G, Cepeda-Díaz AF (1986) Residual shear strength of clays and shales. *Géotechnique* 36:269–274. <https://doi.org/10.1680/geot.1986.36.2.269>

Mesri G, Huvaj-Sarihan N (2012) Residual shear strength measured by laboratory tests and mobilized in landslides. *J Geotech Geoenvir* 138(5):585–593

Mesri G, Shahien M (2003) Residual shear strength mobilized in first-time slope failures. *J Geotech Geoenvir Eng* 129(1):12–31

Mitchell JK (1976) Fundamentals of soil behavior, 1st edn. Wiley, New York

Muir Wood D (1990) Soil behaviour and critical state soil mechanics. Cambridge university press

Palmeira EM, Milligan GW (1989) Scale effects in direct shear tests on sand. *Proceedings of the 12th international conference on soil mechanics and foundation engineering*, Vol. 1, No. 1, pp. 739–742

Pásek J, Janek J, Hroch Z, Francěk J (1972) Engineering Geological Survey of D8 Motorway in part Chotiměř–Radečín, km 62.2–67.8, II. stage. Final Report of Geological Institute of Czechoslovak Academy of Sciences Praha (in Czech)

Pospisil P, Rapantova N, Kyčl P, Novotny J (2019) Pitfalls in generating an engineering geological model, using a landslide on the D8 motorway near Dobkovičky, Czech Republic, as an example. In: IAEG/AEG Annual Meeting Proceedings, San Francisco, California, 2018—Volume 6 (pp. 269–276). Springer, Cham

Roháč J, Kyčl P, Boháč J, Mašín D (2017) Shear strength of soils from the Dobkovičky landslide in the Central Bohemian uplands determined by laboratory tests. *Acta Polytechnica CTU Proceedings* 10:48–51, 2017. <https://doi.org/10.14311/APP.2017.10.0048>

Scaringi G (2016) Influence of pore fluid composition on clay behaviour and chemo-mechanical study of a clayey landslide. Doctoral dissertation, University of Basilicata, Potenza, Italy. <https://doi.org/10.13140/RG.2.2.32935.24486>

Scaringi G, Di Maio C (2016) Influence of displacement rate on residual shear strength of clays. *Proced Earth Planet Sci* 16:137–145. <https://doi.org/10.1016/j.proeps.2016.10.015>

Scaringi G, Telesca G, Vassallo R, Di Maio C (2013) Resistenza residua a taglio di un-argilla illitica: influenza della velocità di scorrimento, della composizione del fluido interstiziale, della modalità di taglio. *Incontro Annuale dei Ricercatori di Geotecnica*, 6 pp (in Italian)

Scaringi G, Fan X, Xu Q, Liu C, Ouyang C, Domènec G, Yang F, Dai L (2018a) Some considerations on the use of numerical methods to simulate past landslides and possible new failures: the case of the recent Xinmo landslide (Sichuan, China). *Landslides* 15:1359–1375. <https://doi.org/10.1007/s10346-018-0953-9>

Scaringi G, Hu W, Xu Q (2018b) Discussion on: "Experimental study of residual strength and the index of shear strength characteristics of clay soil" [Eng.Geo.233:183–190]. *Eng Geol*. <https://doi.org/10.1016/j.enggeo.2018.06.021>

Scaringi G, Hu W, Xu Q, Huang R (2018c) Shear-rate-dependent behavior of clayey bimaterial interfaces at landslide stress levels. *Geophys Res Lett* 45:766–777. <https://doi.org/10.1002/2017GL076214>

Schofield A, Wroth P (1968) Critical state soil mechanics. McGraw-Hill London

Seyček J (1978) Residual shear strength of soils. *Bull Int Assoc Eng Geol-Bull Assoc Int Géologie Ing* 17:73

Skempton AW (1953) The colloidal activity of clays. *Sel Pap Soil Mech*:106–118

Skempton AW (1964) Long-term stability of clay slopes. *Géotechnique* 14:77–102

Skempton AW (1970) First time slides in overconsolidated clays. *Géotechnique* 20(3):320–324

Skempton AW (1977) Slope Stability of cuttings in brown London clay. Proc., 9th Int. Conf. of Soil Mechanics and Foundations, Vol. 3, Springer, New York, pp 261–270

Skempton AW (1985) Residual strength of clays in landslides, folded strata and the laboratory. *Géotechnique* 35:3–18

Sorensen KK, Okkels N (2013) Correlation between drained shear strength and plasticity index of undisturbed overconsolidated clays. In: Proc. 18th ICSMGE, Paris (Vol. 1, pp. 423–428).

Stark TD, Eid HT (1994) Drained residual strength of cohesive soils. *J Geotech Eng* 120:856–871

Stark TD, Hussain M (2013) Empirical correlations: drained shear strength for slope stability analyses. *J Geotech Geoenvir* 139(6):853–862

Stark TD, Choi H, McCone S (2005) Drained shear strength parameters for analysis of landslides. *J Geotech Geoenvir Eng* 131(5):575–588

Stemberk J, Mašín D, Balek J, Blahút J, Hartvíč F, Chaloupka D, Kadlecík P, Kalinová R, Klimeš J, Král J, Kusák M, Rott J, Rybář J, Špaček P, Táborský P (2016) Analysis of the causes of the landslide on the D8 motorway near Dobkovičky village (in Czech), <https://www.mdcr.cz/Dokumenty/Silniční-doprava/Pozemní-komunikace/Analyza-principu-vzniku-sesuvu-na-dalnici-D8-u-Dobko>. Accessed 30 May 2019

Take WA, Bolton MD (2011) Seasonal ratcheting and softening in clay slopes, leading to first-time failure. *Géotechnique* 61(9):757

Tengattini A, Das A, Einav I (2016) A constitutive modelling framework predicting critical state in sand undergoing crushing and dilation. *Géotechnique* 66(9):695–710

Terzaghi K, Peck RB (1948) Soil mechanics in engineering practice. Wiley, New York 566 p

Terzaghi K, Peck RB, Mesri G (1996) Soil mechanics in engineering practice. John Wiley & Sons

Thermann K, Gau C, Tiedemann J (2006) Shear strength parameters from direct shear tests—Influencing factors and their significance. Proceedings of IAEG 2006, The Geological Society of London, Vol. 484, pp. 1–12, London, UK

Tiedemann B (1937) Über die Schubfestigkeit bindiger Böden. Preuß. Versuchsanst. f. Wasserbau u. Schiffbau

Tika TE, Vaughan PR, Lemos LJL (1996) Fast shearing of pre-existing shear zones in soil. *Geotechnique* 46:197–233. <https://doi.org/10.1680/geot.1996.46.2.197>

Tiwari B, Marui H (2005) A new method for the correlation of residual shear strength of the soil with mineralogical composition. *J Geotech Geoenviron Eng* 131:1139–1150

Valečka J (1989) Základní geologická mapa ČSSR 1:25000 (Basic geological map of the CSSR 1:25000), pp. 02–233, Jílové, Czechoslovak Geological Survey, Prague

Voight B (1973) Correlation between Atterberg plasticity limits and residual shear strength of natural soils. *Geotechnique* 23:265–267

Wesley LD (2003) Residual strength of clays and correlations using Atterberg limits. *Geotechnique* 53(7):669–672

Xu C, Wang X, Lu X, Dai F, Jiao S (2018) Experimental study of residual strength and the index of shear strength characteristics of clay soil. *Eng Geol* 233:183–190. <https://doi.org/10.1016/j.engeo.2017.12.004>

Zhang X, Hu W, Scaringi G, Baudet BA, Han W (2018) Particle shape factors and fractal dimension after large shear strains in carbonate sand. *Géotech Lett* 8(1):73–79

**J. Roháč** (✉) · **G. Scaringi** · **J. Boháč** · **J. Najser**

Institute of Hydrogeology, Engineering Geology and Applied Geophysics, Faculty of Science, Charles University, 128 43, Prague, Czech Republic  
Email: jakub.rohac@natur.cuni.cz

**J. Roháč** · **P. Kycl**

Czech Geological Survey, 118 00, Prague, Czech Republic